UNIVERSITÄT
BERN

Oeschger Centre for Climate Change Research (OCCR)

University of Bern

Influence of multi-year La Niña and soil moisture feedback on the Australian Monsoon

Master Thesis, Faculty of Science, University of Bern

handed in by

Quentin Rossier

MSc Climate Sciences

Supervisor
Prof. Stefan Brönnimann

Co-supervisor
Prof. Christoph Raible

Advisor
Ass. Prof. Andréa S. Taschetto

University of Bern - Faculty of Science - Oeschger Centre for Climate Change Research (OCCR)

Abstract

Influence of multi-year La Niña and soil moisture feedback on the Australian Monsoon

by Quentin Rossier

Australian rainfall intensifies during the third year of the triple year La Niña, but the reason for this enhancement is not fully understood. This study investigates the extreme rainfall observed during triple year La Niña in the Australian monsoon region. We show that soil moisture plays a key role in the intensification of the monsoonal circulation. Two hypotheses are evaluated: an inter-monsoonal, multi-year, precipitation enhancement through soil moisture memory; and another one examines an intra-monsoonal enhancement, with earlier rainfall setting an earlier, and intensified, internal monsoonal circulation. The intensification of the internal circulation of the Australian monsoon during triple-year La Niña is also visible in NCAR-CESM2, and MIROC6 models and to a certain extent in the ACCESS-CM2 model. Our findings suggest that the intensification of Australian rainfall occurs one or two months before the usual onset of the monsoon associated with an earlier peak of the third year of La Niña. The increased rainfall in austral spring intensifies soil moisture feedback and increases rainfall recycling in the following season. This intensifies the monsoon season during the third year of triple La Niña.

Contents

Abbreviations

Abbreviation	Meaning
ACCESS-CM2	Australian Community Climate and Earth System Simulator, Coupled Model 2
AUM	Australian Monsoon
AWRA-L v.6	Australian Landscape Water Balance model, version 6
CMIP	Coupled Model Intercomparison Project
CSIRO	Commonwealth Scientific and Industrial Research Organisation
ENSO	El Niño Southern Oscillation
EP	Eastern tropical Pacific Ocean
ERA5	European Centre for Medium-Range Weather Forecasts, reanalysis 5
ERSSTv.5	Extended Reconstructed Sea Surface Temperature, version 5
GCM	General Circulation Models
HadISST	Hadley Centre Global Sea Ice and Sea Surface Temperature
IMC	Internal Monsoonal Circulation
IO	Indian Ocean
IPCC	Intergovernmental Panel on Climate Change
ITCZ	InterTropical Convergence Zone
MIROC6	Model for Interdisciplinary Research on Climate, version 6
MJO	Madden-Julian Oscillation
NA	Northern Australia
NCAR-CESM2	National Center for Atmospheric Research, Community Earth System Model 2
NCI	Australian National Computational Infrastructure
NDJFM	November-December-January-February-March
NOAA	National Oceanic and Atmospheric Administration
ONI	Oceanic Niño Index
SIndo	Southern Indonesia
SO	September and October
SSP1-2.6/SSP5-8.5	Shared Socioeconomic Pathway number 1 or 5, radiative forcing of 2.6 or 8.5 W/m^2
SST	Sea Surface Temperature
WoA	West of Australia

1 Introduction

Most of Northern Australia (NA) experiences above 75% of its annual precipitation between November and March (NDJFM), with a peak occurring in January and February (Figure 1.1). In NA, approximately North from 20°S-25°S (Heidemann et al., 2023; Sekizawa et al., 2023; Yu and Notaro, 2020), this pronounced wet season is attributed to the Australian Monsoon (AUM), a crucial climatic phenomenon of the Australian continent. Year-to-year variability in the AUM rainfall can be strong and have important implications for NA's population, agriculture, and livestock industries which are prominent in these regions (Mollah and Cook, 1996).

The monsoon is characterized by a seasonal reversal of winds and associated rainfall. While its dynamics have been the subject of extensive study, the relationship between the AUM and the El Niño Southern Oscillation (ENSO) remains a subject of significant scientific interest.

1.1 The Australian Monsoon

The AUM's onset is thought to be driven by various factors. The main one is the southward shifts of the InterTropical Convergence Zone (ITCZ), during austral summer. Due to stronger solar radiation in the Southern Hemisphere, the ITCZ shifts southward, following the warm Sea Surface Temperature (SST). The result is a shift of wind patterns over Indonesia and NA, bringing moisture into the Australian continent (Gadgil, 2018).

Another large-scale phenomenon often assimilated with the monsoon is the land-sea thermal wind. The land heats up during spring and summer due to stronger solar radiation. As Australia is warmer than the surrounding ocean, due to lower thermal inertia over the continent, air rises, creating a pressure gradient between land and ocean, and inducing low-level winds from the ocean to Australia. However, the role of the land-sea thermal wind in the monsoon onset has been recently questioned. Indeed, recent studies have shown that stronger differential heating is sometimes related to weaker monsoons (Gadgil, 2018; Geen et al., 2020).

The rainfall during the AUM has a low correlation with the rainfall anomaly of NA during the rest of the year (Sekizawa et al., 2023). This indicates that the AUM operates as an independent system and high rainfall outside the monsoon season does not necessarily predict a strong monsoon. Figure 1.2 shows the circulation patterns usually seen during the AUM season during active phases. The monsoon trough is where low pressure converges, creating convection and rainfall. The AUM is generally separated in two to three monsoon cycles. Each cycle has an active and an inactive phase. During the inactive phase, the monsoon trough moves northward,

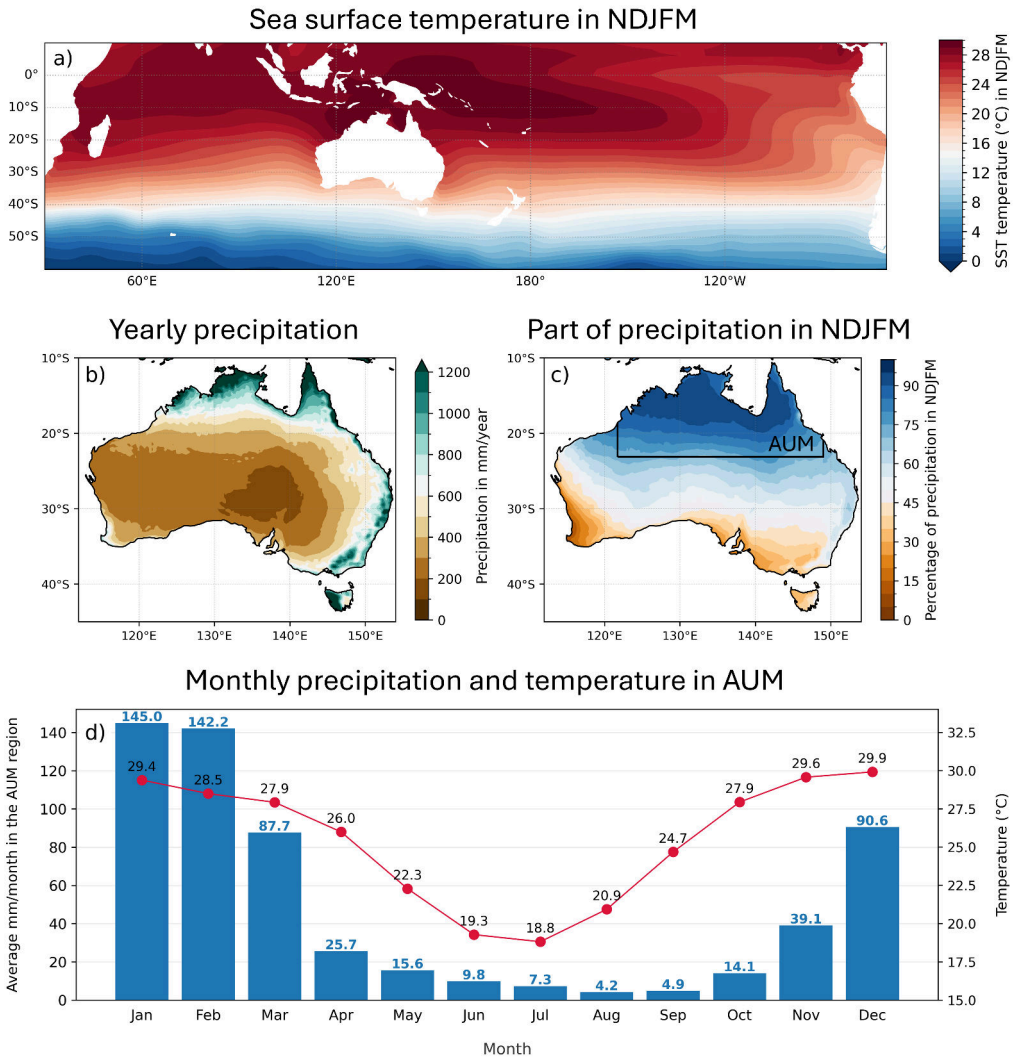

Figure 1.1: a) Sea surface temperature average in NDJFM b) Australian annual mean rainfall in mm. c) Percentage of the yearly precipitation accumulated between November and March. The black box represents the Australian Monsoon region considered in this study. d) Average monthly rainfall in the Australian Monsoon region. The data comes from the ERA5 reanalysis between 1940 and 2023.

and the rainband moves to Indonesia. During the active phase, the monsoon trough goes over NA (Figure 1.2, Hung and Yanai, 2004).

Active phases of the monsoon are marked by bursts, which correspond to the arrival of large-scale weather systems over NA. Bursts are defined as short periods within the monsoon characterized by excessively wet conditions, in contrast to breaks, associated with excessively dry conditions. The rainfall associated with the AUM primarily results from monsoon disturbances propagating across NA. The origin of these disturbances is influenced by external factors, such as extratropical Rossby wave breaking along the eastern coast of Australia (Berry et al., 2012), or the Madden-Julian Oscillation (MJO, Berry and Reeder, 2016).

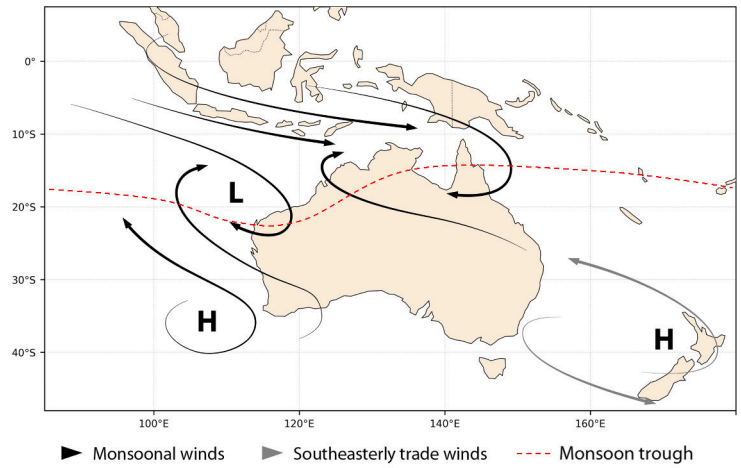

Figure 1.2: Schematic of the circulation patterns typically associated with the AUM in its active phase.

1.2 The ENSO phenomenon

The ENSO phenomenon originates in the Eastern tropical Pacific Ocean (EP) and is known for its capacity to disrupt weather patterns across the globe. During a neutral phase, easterly trade winds flow over the Pacific Ocean, resulting in upwelling on the South American coast and relatively warmer waters in the Western Pacific Ocean, and convective activity and rainfall over there (Figure 1.3). During the La Niña phase, the circulation strengthens with stronger trade winds and more upwelling in the EP. At the surface, the air travels westward where the SST is warmer, in the Western Pacific Ocean. In this region, the air converges and rises, leading to abnormally strong precipitation, while EP encounters drier than usual conditions.

In the case of an El Niño event, there is a weakening or, in extreme cases, reversal of the trade winds in the Pacific Ocean and a slowdown or stopping of the upwelling in the EP. In such an event, SST in the EP rises due to the weak upwelling. The air converges and rises over the warmer SST in the central-eastern Pacific, leading to convection and precipitation over the EP. The rising motion of the air leads to convection and precipitation over the EP, which disrupts the Walker cell. As a result of this disruption, in the upper troposphere, the air, which has lost moisture, travels back to its initial location and descends over Indonesia and South America (Figure1.3). Consequently, this subsidence significantly lowers the precipitation over these regions (Hendon, 2003).

1.2.1 Defintion of La Niña/El Niño events

There are different ways to define La Nina and El Niño events. One of the most common methods is when the SST in the central Pacific surpasses a certain threshold. This temperature anomaly is calculated with many different indices (Niño 1, Niño 3.4,...), but the Oceanic Niño Index (ONI) is the one used by the National Oceanic and Atmospheric Administration (NOAA) to issue ENSO warnings which are widely used by the scientific community (Kousky and Higgins, 2007). The ONI averages the SST between 5°N-5°S, and 120°-170°W (NOAA, 2023). For instance,

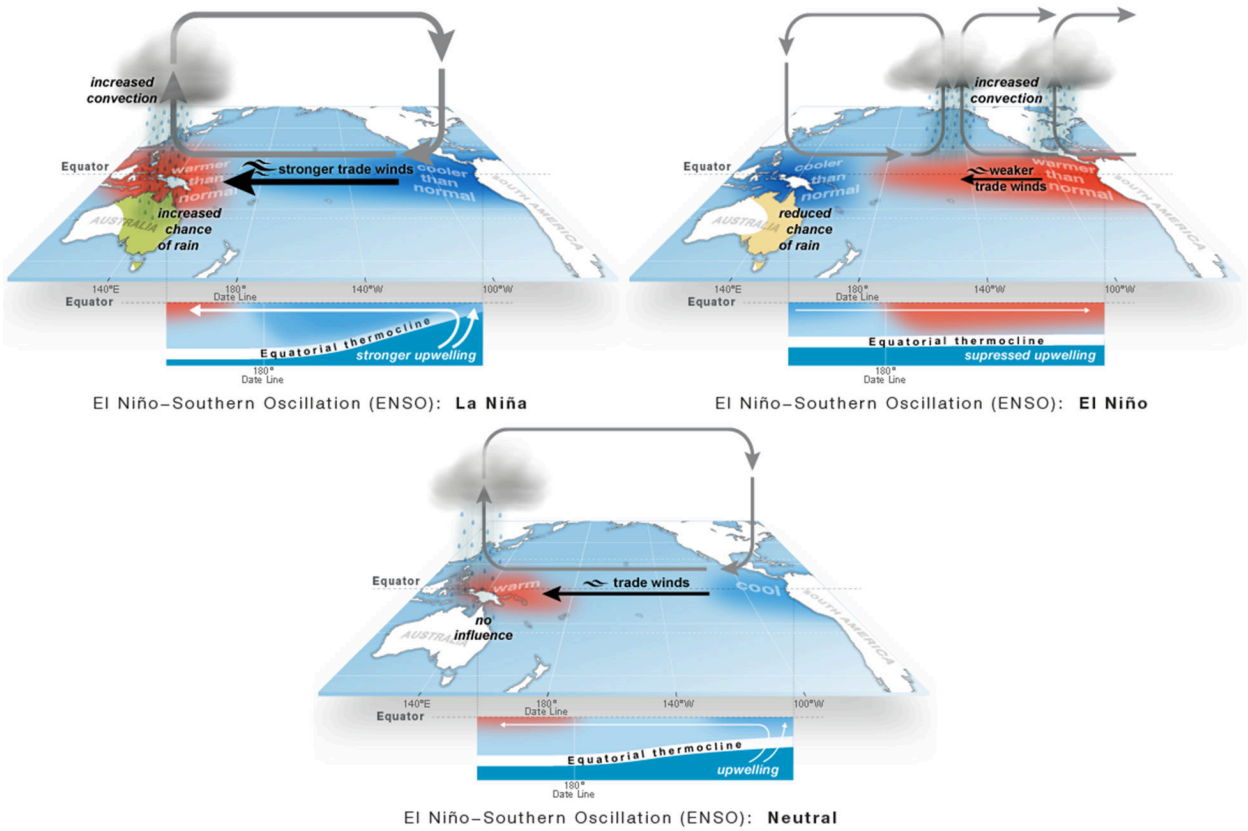

Figure 1.3: Scheme of ENSO interaction between the SST and the Walker cell (Australian Bureau of Meteorology, n.d.-a).

the NOAA sets the La Niña (El Niño) warning when five consecutive overlapping seasons have a temperature lower than -0.5°K (higher than +0.5°K). ENSO tends to be highly irregular and can result in two consecutive years of La Niña or El Niño, or even three consecutive years in rarer cases. Since 1940, three consecutive years of La Niña events have happened three times (in 1973-76, 1998-2001, and 2020-2023). Double events in La Niña are more common than double El Niño events, as they have happened in about 50% of La Niña events (Figure 1.4). On the other hand, triple El Niño events are uncommon due to ENSO asymmetry (Dommenget et al., 2013), and only one triple event has been recorded since 1940 (1939-1942)

Indeed, although El Niño events are typically more intense than the La Niña events, they tend to dissipate sooner. This is due to the low-level wind forcing from the Indian Ocean (IO) on the Western Pacific Ocean, counteracting and slowly terminating the El Niño events (Okumura and Deser, 2010). The duration of El Niño events is mainly phased to the seasonal cycle and on the timing of its onset, whereas the duration of a La Niña is more linked to the strength of the warm event preceding. Therefore, a La Niña can be longer than an El Niño (Wu et al., 2019), and multi-year La Niña can be influenced by a strong El Niño event preceding (DiNezio et al., 2017).

The most recent projection of ENSO in a warming climate tends to indicate that stronger El Niño and more multi-year La Niña will occur during the twenty-first century (Cai et al., 2021). Multi-year La Niña can lead to a reinforcement of the rainfall patterns as seen in the USA (Okumura et al., 2017) but they can also lead to

diverse patterns between the first and the second year of the event as seen in South America (Lopes et al., 2022).

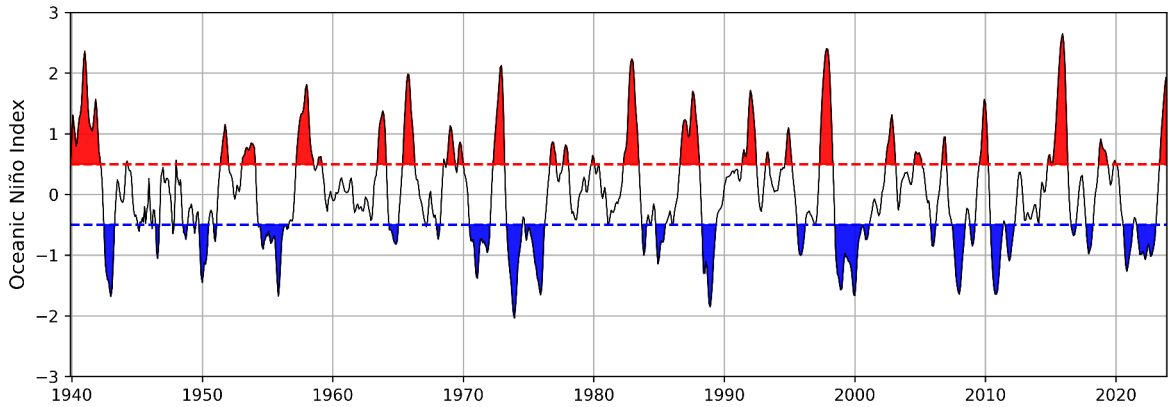

Figure 1.4: ONI since 1940 with ERSSTv.5 SST reanalysis. In blue are La Niña events and in red are El Niño events.

1.2.2 Influence of ENSO on the Australian climate

ENSO has a very important impact on the interannual rainfall variability of the Australian continent. ENSO directly impacts NA through a difference in pressure linked to this phenomenon. This pressure change has been identified and measured since the 1870s with the Southern Oscillation Index, representing the difference in pressure between Darwin and Tahiti (Australian Bureau of Meteorology, n.d.-a). Southeast Australia is also widely impacted by ENSO but in an indirect way. Indeed, ENSO's influence is felt for instance through Rossby wave trains (Cai et al., 2012; Gillett et al., 2023) and the Southern Annular Mode (Hendon et al., 2014). During El Niño events, southern Australia is usually experiencing warmer than usual temperatures. In eastern Australia, reduced precipitation is generally seen (Australian Bureau of Meteorology, n.d.-a). In extreme cases, the Australian continent can be hit by severe drought conditions and heatwaves over a large part of the country (Chiew et al., 1998). During La Niña events, higher rainfall tends to occur in spring in most of Australia, and colder temperatures are recorded in the South (Australian Bureau of Meteorology, n.d.-a).

The impact of ENSO is generally stronger during winter and spring seasons as the large-scale atmospheric circulation is more prone to Rossby wave generation and propagation (Gillett et al., 2023). Multi-year ENSO events also play a role on the Australian continent. Indeed, second-year El Niño events are drier than average El Niño in the center and northern part of the continent in summer. Third-year La Niña events seem to produce extreme conditions, with strong precipitation in northern and eastern Australia (A. T. Huang et al., 2024).

The shape of the ENSO event also has an impact on the Australian climate (Freund et al., 2021; Taschetto et al., 2009; Taschetto and England, 2009). Indeed, studies have shown that ENSO events acting on the central Pacific Ocean have a different impact on the precipitation than ENSO events developing in the EP. During strong central Pacific El Niño, Australia tends to be drier during winter and early spring. However,

from October, more rainfall is recorded in the southeastern regions (Freund et al., 2021).

1.3 Different mechanisms affecting AUM rainfall variability

AUM rainfall has strong interannual variability, up to 80% difference between the years (Sekizawa et al., 2023). Much research has been done to identify the reasons for such an important variability. A part of this variation can be attributed to the ENSO phenomenon. However, ENSO is not the only process that influences the AUM. The AUM is affected by many internal and external processes, making it very complex to predict.

1.3.1 ENSO

The consequences of an El Niño on the AUM have been well-documented since the 1980s (McBride and Nicholls, 1983) and often lead to lower-than-average AUM rainfall. A stronger El Niño event does not necessarily mean a drier than usual AUM (Figure 1.5), but it reduces the chances of wet events. Indeed, compared to a weak El Niño, a strong El Niño does not necessarily lead to a drier AUM (as shown by the yellow linear regression in 1.5) but it reduces the likelihood of above-average AUM rainfall (McGregor et al., 2024; Tozer et al., 2023). Conversely, La Niña events are associated with anomalously wet conditions and stronger La Niña tends to result in more abundant AUM rainfall (Figure 1.5, Chung and Power, 2017). It has been shown that northeastern Australian rainfall tends to be more correlated to ENSO than northwestern Australian one due to its direct proximity with the Pacific Ocean (Sharmila and Hendon, 2020). The ENSO phenomenon is the atmospheric feature that explains most of NA rainfall variability with a correlation of -0.57 (Figure 1.5). This correlation can vary depending on the region and the ENSO index used (Tozer et al., 2023).

The AUM onset is also widely influenced by ENSO. Indeed, during an El Niño (La Niña) phase, the onset of the AUM is usually later (earlier) than average (Australian Bureau of Meteorology, n.d.-d). Examining the rainfall and ONI during the extended austral summer (NDJFM), we observe that a stronger La Niña often correlates with heavier rainfall (Figure 1.5). However, the three third-year La Niña recorded since 1940 are well above what linear regression suggests, although they were linked with weaker La Niña, indicating the influence of other factors.

As seen earlier, central and eastern ENSO events can lead to various rainfall patterns in Australia. Those different events also affect the AUM region (Taschetto et al., 2009; Taschetto and England, 2009). For instance, El Niño events located in central Pacific Ocean, also known as El Niño Modoki (Ashok et al., 2007), are generally associated with a decrease in rainfall in northwestern and NA, with a stronger decrease in austral autumn (Taschetto and England, 2009).

1.3.2 The Indian Ocean

While the Pacific Ocean SST patterns explain in part the AUM rainfall variability with ENSO and the Interdecadal Pacific Oscillation, the IO, also plays a major role in the AUM. As a direct influence of the IO, most of the moisture brought over NA

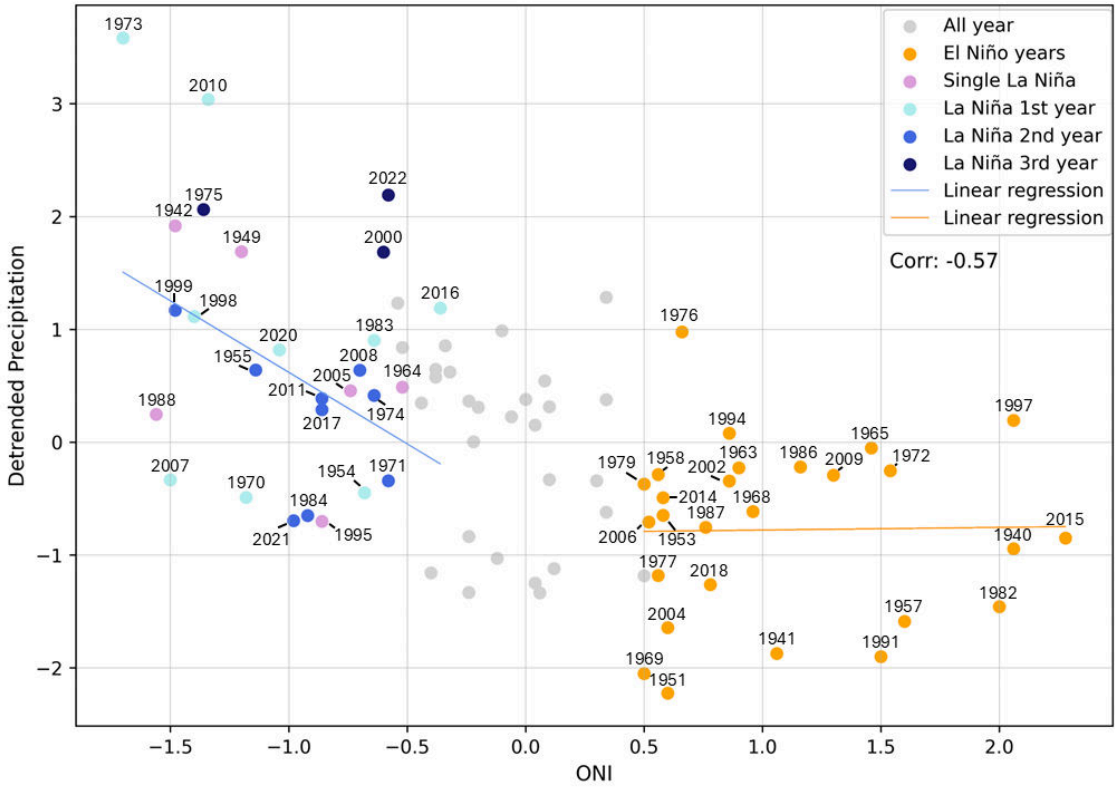

Figure 1.5: Scatter plot of the ONI in NDJFM and the detrended precipitation (in mm/day) in the AUM region in NDJFM since 1940. As a monsoon straddles two years, only the first year is written here. The AUM region, the ONI, and the detrending process are described in section 2.4. The data used are detailed in section 2.3

during the AUM comes from the IO (Figure 1.2, Holgate et al., 2020). For example, wind-evaporation feedback over the Southeastern IO is an important feature of the AUM (Sekizawa et al., 2018).

The IO basin-wide warming (Chambers et al., 1999) also influences the AUM. During an El Niño event, anomalous subsidence is observed over NA and Indonesia (Figure 1.3). This subsidence strengthens the trade winds over the eastern IO, which in turn enhances upwelling in this region. The resulting upwelling often leads to a positive IO dipole, characterized by cooler SST in the eastern IO and warmer SST in the western IO. This SST gradient across the IO induces an easterly flow that can delay the onset of the AUM (Heidemann et al., 2023). However, once the AUM begins, the winds reverse (Figure 1.2), halting the upwelling and advecting warm water into the eastern IO, creating a basin-wide warming. When this IO basin-wide warming appears after an El Niño event, AUM rainfall tends to decrease (Taschetto et al., 2011).

1.3.3 Terrestrial processes

Soil moisture plays a crucial role in the climate through its impact on water and energy cycles. In case of high soil moisture, the energy induced by solar radiation is more likely to be transformed into latent heat through evaporation. The enhanced moisture in the atmosphere can trigger more convection and therefore more precipitation (Bui et al., 2023). Previous studies have shown that soil moisture can affect monsoons, with a deeper and stronger low-pressure coming inland when soil moisture is higher than average (Berg et al., 2017; Hunt and Turner, 2017). This land-ocean-atmosphere interaction is also considered to be relatively important during the AUM, especially in northwestern Australia (Bui et al., 2023; Sharmila and Hendon, 2020). Recent research have shown that around 25% of the monsoonal rainfall are coming from terrestrial contribution (Holgate et al., 2020).

In their research, Sekizawa et al. (2023) show that soil moisture at the beginning of February has a stronger correlation with February-mean rainfall than the correlation between February-mean rainfall and January-mean rainfall. It suggests that soil moisture may positively influence the subsequent precipitation anomalies. This indicates that while previous precipitation affects soil moisture, the current soil moisture conditions can enhance the persistence of rainfall anomalies.

There is also a link between soil moisture and rainfall over the years, especially in northwestern Australia. Indeed, Sharmila and Hendon (2020) have demonstrated that over a 5-year period, the variability of the AUM appears to be primarily influenced by interactions between soil moisture and precipitation, as well as a localized feedback loop involving precipitation, wind, and evaporation. Furthermore, terrestrial processes such as leaf area index and soil moisture are believed to account for 21% to 36% of the variation of the AUM rainfall between January and March, considerably more than oceanic influences, which represent 14% of this variation (Yu and Notaro, 2020). Additionally, Martius et al. (2021) demonstrated that adding soil moisture across the Australian continent during summertime results in lower temperatures and higher precipitation over NA.

1.3.4 Other factors influencing the AUM rainfall variability

Other large-scale atmospheric phenomena can influence the onset or burst of the AUM. We can cite the MJO which is an eastward-moving system of convective activity that propagates through the tropical regions, generally along the ITCZ (Madden and Julian, 1972). It is described as "a pulse of wind, enhanced cloud, and rainfall that cycles eastwards around the globe near the equator." (Australian Bureau of Meteorology, n.d.-b). It can occur at any moment of the year and has a life cycle between 30 to 60 days. The MJO has eight phases, which depend on its location. It usually emerges over Africa or the western IO and shifts eastward above NA after two or three weeks. It then shifts toward the Pacific Ocean and South America. During phases 4 and 5, the MJO is between the eastern IO and the western Pacific Ocean, the perfect longitude to transport moisture above NA, which stimulates the onset and burst of the AUM (Australian Bureau of Meteorology, n.d.-c; Hung and Yanai, 2004; Yu and Notaro, 2020).

Another factor influencing the onset of the AUM is the Convectively Coupled Equatorial Waves (Ida et al., 2020) which is similar to the MJO, except that it has a weaker signal and is generally associated with westward motion. The mid-latitude trough intrusions also play an important role in the AUM, especially during bursts (Berry and Reeder, 2016; S. Narsey et al., 2017).

Oceanic multi-decadal variability has an important impact on the AUM as well. The positive, or negative, phase of the Interdecadal Pacific Oscillation is important in the response of the Australian rainfall depending on the ENSO phase (Heidemann et al., 2022). The Australian rainfall - ENSO relationship is usually stronger during the negative phase of the Interdecadal Pacific Oscillation (Power et al., 1999). Also, past positive events have coincided with lower AUM rainfall.

1.4 Past and future trends of the AUM

Between 1920 and 2021, there was an increase in the AUM region of 18mm per decade of precipitation (Heidemann et al., 2023) between December and March. This trend has accelerated since 1950, with an average of 24mm per decade. In northwestern Australia, the acceleration is even stronger in austral summer, with some areas having more than 50 mm per decade increase (Dey et al., 2019). Furthermore, the duration of the wet season has lengthened over time, with an important increase of 3.4 days per decade (Uehling and Misra, 2020). However, in some northeastern regions, there are almost no changes in precipitation or the length of the AUM, especially along the coast.

There has been growing interest in understanding this rainfall increase for long-term planning and mitigating the possible impacts of extreme events associated with it as the climate warms. Due to this increasing trend, northwestern Australia tends to have earlier monsoon onset with more frequent westerly bursts, tropical cyclones, and monsoon lows (Heidemann et al., 2023). The reasons for those changes can be diverse. Research by Ha et al. (2020) shows that the high concentration of anthropogenic aerosols over Asia induces a North-South thermal gradient. This thermal

gradient leads to a southward flow, bringing more rainfall over the AUM. Other factors could influence this rainfall enhancement such as the warming of the western Pacific Ocean (Roxy et al., 2019) and the warming of the tropical Atlantic Ocean (Lin and Li, 2012).

Due to greenhouse gas emissions, the Australian climate is changing fast. It is important to use climatic models to understand the climate and to predict it. The most accurate simulations of the climate come from the models part of the Coupled Model Inter-comparison Project phase six (CMIP6). They incorporate the latest advancements in understanding the Earth's climate system and are part of the latest Intergovernmental Panel on Climate Change (IPCC). The CMIP6 models provide a standardized framework for results across research groups, improving the reliability of climate projections on both global and regional scales. In the CMIP6 there are 23 models with each one there bias in the representation of the climate. The general representation of the Australian climate by the CMIP6 models also shows some biases, with precipitation higher than in reanalysis over the center, and lower than in reanalysis along the eastern coast and in NA (Grose et al., 2020). Despite persistent biases, there has been an overall improvement from CMIP5 to CMIP6 to represent Australian rainfall and its relationship with climate modes of variability (Chung et al., 2023; Grose et al., 2020)

CMIP5 and CMIP6 models on a very high fossil fuel scenario, with a radiative forcing of $8.5 W/m^2$ (SSP5-8.5), show a decrease in precipitation on the western coast and an increase on the southeast coast during summer and autumn. In winter and spring, rainfall is projected to decrease strongly on the western and eastern coasts (Grose et al., 2020). CMIP5 and CMIP6 models show a low agreement concerning rainfall over the AUM region. By 2100, half of the CMIP6 models project a decrease and the other half an increase in precipitations in the AUM (S. Y. Narsey et al., 2020). Due to global warming, temperatures over the AUM region are projected to rise four to five degrees by 2100, compared to the mean for 1995-2014 (SSP5-8.5). Stronger precipitation bursts are projected, with annual maximum one-day rainfall increasing by five to twenty millimeters over NA (Grose et al., 2020). With lower fossil fuel usage scenarios (SSP1-2.6), no significant increase or decrease in precipitation can be seen in the CMIP6 models (Lee et al., 2021).

2 Article - Influence of multi-year La Niña and soil moisture feedback on the Australian Monsoon

The following article was submitted to the Journal of Climate on the 10th of October 2024. The figures' number as well as the layout has been changed for this thesis. The whole text has been written by myself and has been rewarded and corrected by the two co-authors Ass. Prof. Andréa S. Taschetto and Prof. Stefan Brönnimann.

2.1 Abstract

Australian rainfall intensifies during the third year of the triple year La Niña, but the reason for this enhancement is not fully understood. This study investigates the extreme rainfall observed during triple year La Niña in the Australian monsoon region. We show that soil moisture plays a key role in the intensification of the monsoonal circulation. Two hypotheses are evaluated: an inter-monsoonal, multi-year, precipitation enhancement through soil moisture memory; and another one examines an intra-monsoonal enhancement, with earlier rainfall setting an earlier, and intensified, internal monsoonal circulation. The intensification of the internal circulation of the Australian monsoon during triple-year La Niña is also visible in NCAR-CESM2, and MIROC6 models and to a certain extent in the ACCESS-CM2 model. Our findings suggest that the intensification of Australian rainfall occurs one or two months before the usual onset of the monsoon associated with an earlier peak of the third year of La Niña. The increased rainfall in austral spring intensifies soil moisture feedback and increases rainfall recycling in the following season. This intensifies the monsoon season during the third year of triple La Niña.

2.2 Introduction

The Australian monsoon (AUM) is an important climatic feature of the Australian continent. It traditionally spans during the austral summer months, typically commencing around November and continuing until March (NDJFM). During the monsoon, most of Northern Australia (NA) receives more than 75% of its annual precipitations (Figure 2.1). During the austral summer, the InterTropical Convergence Zone (ITCZ) shifts south following the intensification of solar radiation in the Southern Hemisphere. This displacement of the ITCZ and the resulting meridional shift in the Hadley circulation alter the wind patterns favoring a reversal of the wind from southeastern to northwestern over NA. This sudden change creates a zone of convergence and a low-level cyclonic circulation over NA (Figure 2.2). This cyclonic

circulation transports moisture from the southeastern Indian Ocean and creates the AUM.

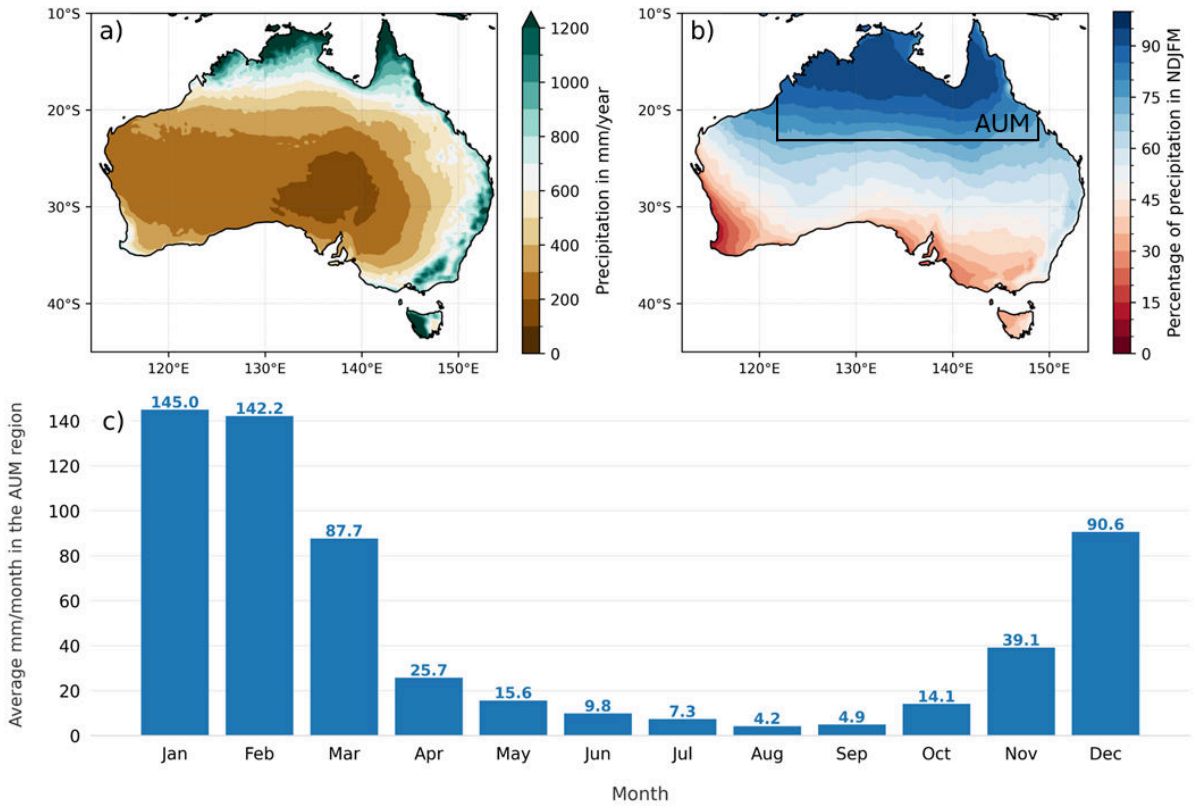

Figure 2.1: a) Australian mean annual rainfall in mm. b) Mean percentage of the yearly precipitation accumulated between November and March. The black box represents the Australian Monsoon region considered in this study. c) Climatology of monthly rainfall averaged in the Australian Monsoon region. The data comes from the ERA5 reanalysis between 1940 and 2023.

Year-to-year variations in the AUM rainfall can have important implications for the local population, agriculture, and livestock industry which are prominent in NA (Mollah and Cook, 1996). Furthermore, the AUM variability can influence other regions' climates. For instance, the variability in AUM can significantly affect the severity of the East Asian winter climate, resulting in notable anomalies in temperature and precipitation across East Asia and the Western North Pacific (Sekizawa et al., 2021). Understanding and assessing these interactions and climatic repercussions is essential for both regional and global climates.

While the dynamics of the AUM variability have been the subject of extensive research, the relationship between the AUM and El Niño Southern Oscillation (ENSO) events remains a subject of significant scientific interest. It is known that Australian rainfall is strongly associated with ENSO (Heidemann et al., 2023; McBride and Nicholls, 1983). The influence of ENSO on Australian rainfall varies seasonally, being more consistent during austral winter and spring (McBride and Nicholls, 1983). During summer, this relationship is generally weaker as it varies substantially depending on ENSO types (Freund et al., 2021; A. T. Huang et al., 2024; Taschetto et al., 2009; Taschetto et al., 2010), multidecadal oscillations (Heidemann et al., 2022, 2023),

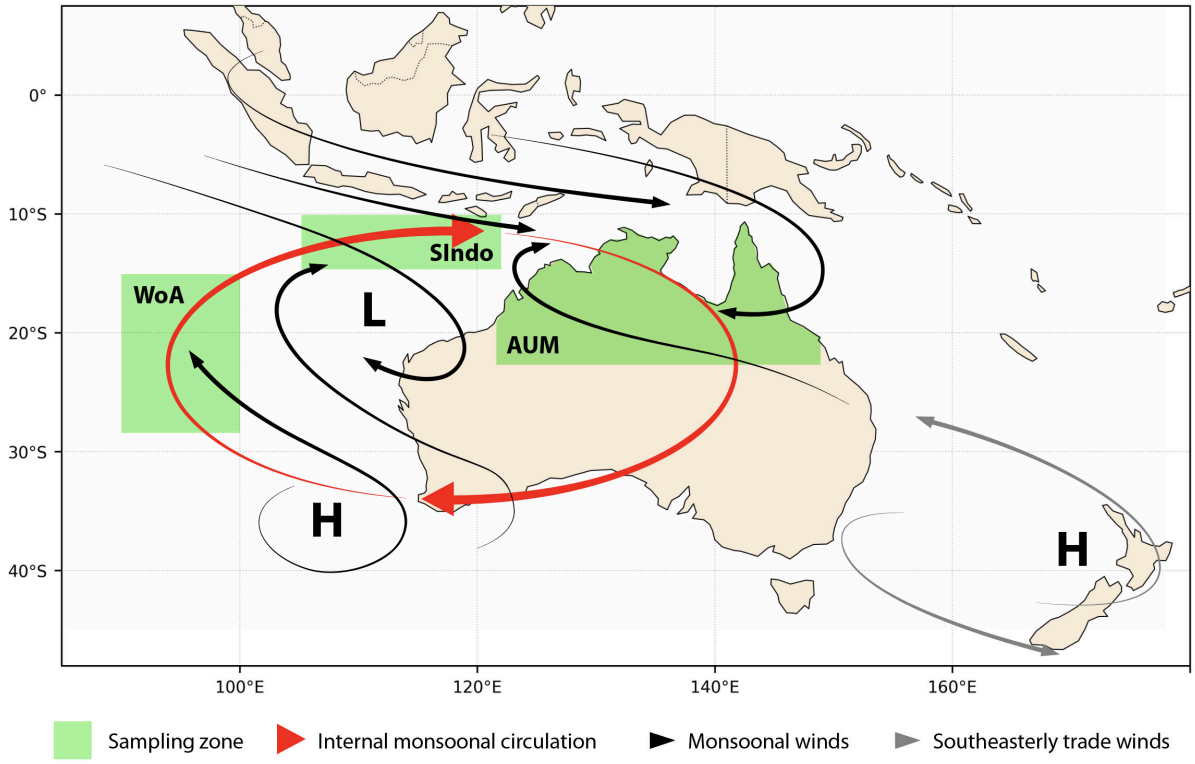

Figure 2.2: Schematic of the circulation patterns typically associated with the Australian monsoon. In red the internal monsoonal circulation such as described by Sekizawa et al. (2023) and in green the sampling zone.

and nearby air-sea and local land-atmosphere feedbacks (Hendon, 2003; Sharmila and Hendon, 2020). In addition, the ENSO - Australian rainfall relationship is asymmetric with La Niña having a stronger influence on rainfall than El Niño (Chung and Power, 2017; Power et al., 2006). During La Niña events, Australia typically experiences more rainfall as temperatures in the Central Pacific get lower (Figure A1).

Multi-year La Niña can have diverse effects on regional climate. For instance, Okumura et al. (2017) show that it can reinforce precipitation patterns in the USA. It can also lead to different patterns between the first and second year of La Niña as seen in South America (Lopes et al., 2022). A recent study by A. T. Huang et al. (2024) has shown that very intense rainfall occurs generally in the third year of La Niña in the eastern and northern parts of Australia during austral spring and summer. The reasons for this rainfall enhancement are unclear since La Niña is generally weaker in the last year of multi-year events, and this is what we aim to investigate in this study.

In addition to ENSO, local processes can also have an impact on the AUM, such as soil moisture. Indeed, previous studies have shown that soil moisture can affect monsoons, with usually deeper and stronger low-pressure developing over NA when soil moisture is high (Rahmati et al., 2024; Timbal et al., 2002). This land - atmosphere interaction plays an important role in modulating the AUM rainfall, especially in northwestern Australia (Holgate et al., 2020; Sharmila and Hendon,

2020). Sekizawa et al. (2023) show a stronger correlation between soil moisture on the first of February and February rainfall than between January rainfall and February rainfall. This suggests that rainfall in the second part of the monsoon period depends more on soil moisture than on large-scale atmospheric systems. This intra-monsoonal rainfall enhancement occurs through localized feedback, where increased soil moisture leads to higher evaporation rates and further precipitation. A soil moisture influence in year-to-year rainfall has been suggested to exacerbate rainfall in northwestern Australia (Sharmila and Hendon, 2020), leading to inter-monsoonal rainfall enhancement as well. This inter-monsoonal rainfall enhancement is not a feature seen for every monsoon system (Douville et al., 2007; Rahmati et al., 2024). Soil moisture recycling significantly impacts Australian rainfall, particularly in the northwestern and southeastern regions (Holgate et al., 2020). It is estimated that, during summer, terrestrial processes account for 21% to 36% of the variation of the AUM rainfall, considerably more than oceanic influences, which represent 14% of its variation (Holgate et al., 2020; Yu and Notaro, 2020).

During years with strong rainfall, an Internal Monsoonal Circulation (IMC) can appear over Australia and Eastern Indian Ocean. This IMC is driven by enhanced convective heating over NA, which creates low-pressure areas that intensify monsoonal winds. This process is further supported by wind-evaporation feedback, where increased oceanic evaporation from the southeastern Indian Ocean supplies moisture to sustain convection. Additionally, soil moisture memory contributes to the persistence of rainfall anomalies, reinforcing the internal dynamics of the AUM system (Sekizawa et al., 2023). This mechanism described by Sekizawa et al. (2023) is independent from ENSO. Here we show that a similar mechanism can operate on the last year of multi-year La Niña events.

This study investigates the increased Australian rainfall in multi-year La Niña. Our hypothesis is separated into two parts. The first one is an inter-monsoonal enhancement via land-atmosphere positive feedback involving rainfall and soil moisture memory in the third year of triple La Niña events. The second part is an intra-monsoonal enhancement of the IMC within the same monsoon season, similar to Sekizawa et al. 2023 mechanism. We show that the two hypotheses are compatible with each other, and suggest they are linked. As recent projections of ENSO in a warming climate indicate increased ENSO variability and higher occurrence of multi-year La Niña events will occur in the near future (Cai et al., 2021; Geng et al., 2023), it is crucial to understand the mechanisms that lead to increased AUM for a better management of the water and the agriculture in NA.

The rest of the study is organized as follows: Section 2.3 describes the data analyzed and the models used; Section 2.4 details the methods used for this research; Section 2.5 describes and discusses the monsoonal changes during multi-year La Niña events, as seen in the reanalysis and the models; And finally, Section 2.6 concludes this research.

2.3 Data

2.3.1 Observations and reanalysis

To investigate the mechanisms involved in the interaction between multi-year La Niña and the AUM, different fields in the atmosphere, ocean, and land are analyzed. Those fields are necessary to identify patterns between consecutive years of La Niña, how they differ from the mean state, and explore possible feedback happening between land, atmosphere, and ocean.

ERA 5

We use the gridded reanalysis from the European Centre for Medium-Range Weather Forecasts (ERA5) to analyze monthly mean atmospheric fields during La Niña events. ERA5 is available from 1940 to 2024, so our analysis concentrates on this period. The ERA5 combines model data with observations to create 4D-Var assimilation fields and model forecasts based on the Integrated Forecasting System Cy41r2. ERA5 has a horizontal resolution of 0.25 x 0.25 degrees for the atmosphere and 137 vertical levels up to 80 km (Hersbach et al., 2023). The variables used here are: horizontal wind at 10 m height, taken to understand the different patterns of the AUM and its changes during multi-year La Niña; evaporation and vertically integrated moisture divergence, studied to better understand the land-ocean-atmosphere feedback, and identify the different sources of humidity enhancing the AUM; sea level pressure, used to understand the underlying mechanisms of the AUM interaction with the ENSO; temperature is assessed, as it could play a role in the setting the monsoon, and modulating water vapor in the atmosphere and, finally, precipitation, which is used to quantify the importance of the AUM rainfall and its variability.

ERSSTv.5

Monthly Sea Surface Temperature (SST) from the National Oceanic and Atmospheric Administration (NOAA) Extended Reconstructed SST, version 5 (ERSSTv.5) dataset is used in this study to better understand the feedback between wind, evaporation, and SST over the southeastern Indian Ocean and its consequences on the AUM rainfall during a multi-year La Niña. It is also used to calculate the Oceanic Niño Index (ONI). The ERSSTv.5 dataset starts in 1854 and is based on a 2 x 2 degrees grid (B. Huang et al., 2017). The ERSSTv.5 reconstruction was chosen over the Hadley Centre Global Sea Ice and Sea Surface Temperature (HadISST; Titchner and Rayner, 2014) to be consistent with the SST data used in the NOAA for the ONI. The ERSSTv.5 is available at https://psl.noaa.gov/data/gridded/data.noaa.ersst.v5.html. However, both datasets are similarly accurate (B. Huang et al., 2018) and give similar ENSO events, except for a slightly smaller variability in the ONI during the early 20th century in the HadISST (Figure A2).

AWRA-L v.6

For the soil moisture, we use the Australian Landscape Water Balance model (AWRA-L v6, available via https://github.com/awracms/awra_cms). This model takes the daily precipitation and temperature information provided by the Australian Water Availability Project (AWAP) on a 0.05 x 0.05 degrees grid and reconstructs Australia's water resources from 1911 until now (Frost et al., 2018). In AWRA-L v6 the monthly

soil moisture is given in cubic meters of water present per cubic meter of soil in the first meter of the soil.

2.3.2 Climate models

Both observational data and reanalysis have limited sample size, as only a few multi-year La Niña have been observed since 1940 (A. T. Huang et al., 2024). Therefore, it is important to look at models to test our hypothesis. For this research, we use the preindustrial control run of three General Circulation Models (GCM) to investigate the AUM rainfall variability. These global models are readily available at the Australian National Computational Infrastructure (NCI) facility at the time of this analysis and they are part of the sixth Coupled Model Intercomparison Project (CMIP6, Eyring et al., 2016). They also represent each one specific characteristics of ENSO, important for the analysis of multi-year La Niña. The preindustrial control run is a fully coupled simulation that does not take into account external forces such as greenhouse gases or aerosols. This way this run allows us to investigate the natural processes related to internal variability of the climate system without the interference of external forcing which complicates the interpretation of the mechanisms behind ENSO and Australian rainfall relationship. In addition, each of these runs provides between 500 and 1200 years of simulation allowing for a large sample size of multi-year ENSO events.

ACCESS-CM2

The Australian Community Climate and Earth System Simulator, Coupled Model 2 (ACCESS-CM2) is a GCM developed by the Australian Bureau of Meteorology, and the Commonwealth Scientific and Industrial Research Organisation (CSIRO). The ACCESS-CM2 includes atmosphere, land, ocean, and sea-ice components as detailed in Table 1 (Dix et al., 2019). The ACCESS-CM2 is one of the best when it comes to the simulation of the amplitude, the structure, and the seasonality of ENSO (Figure A3, Hou and Tang, 2022, Planton et al., 2021). This model also adequately represents the teleconnection between ENSO and the Australian rainfall (Chung et al., 2023). It is well known that the ACCESS-CM2 has a marked biennial ENSO (Rashid et al., 2022), which could complicate its accuracy in recreating triple-year La Niña events.

MIROC6

The Model for Interdisciplinary Research on Climate (MIROC) model is also part of the CMIP6 initiative. The sixth version of this model is provided by the Japan Agency for Marine-Earth Science and Technology, the Atmosphere and Ocean Research Institute at the University of Tokyo, the National Institute for Environmental Studies, and the Institute of Physical and Chemical Research (RIKEN) Center for Computational Science. It was released in 2017 and presents the components seen in Table 1 (Tatebe and Watanabe, 2018). This model has been shown to be one of the best CMIP6 models when it comes to the representation of the amplitude and asymmetry of the interannual variability of ENSO. It also recreates well the magnitude of La Niña (Zhao and Sun, 2022). As we aim for a realistic representation of La Niña phenomena, and its interannual variability the MIROC6 seems to be well suited for the analysis.

TABLE 1: Component of the different model used with their horizontal and vertical resolution.

Component and lon/lat – levels / Models	ACCESS-CM2	MIROC6	NCAR-CESM2
Aerosols / Chemical processes	UKCA-GLOMAP-mode 192x144 85 levels	SPRINTARS6.0 256x128 81 levels	MAM4 288x192 (0.9°x1.25°) 32 levels
Atmospheric processes	MetUM-HadGEM3-GA7.1 192x144 85 levels	CCSR AGCM 256x128 81 levels	CAM6 288x192 32 levels
Land processes	CABLE2.5 192x144	MATSIRO6.0 256x128	CLM5 288x192
Land ice	-	-	CISCM2.1 320x384 with varying grid 60 levels
Ocean processes	GFDL-MOM5 360x300 (tripolar grid) 50 levels	COCO4.9 360x256 (tripolar grid) 63 levels	POP2 320x384 with varying grid 60 levels
Biochemical processes	-	-	MARBL 320x384 with varying grid 60 levels
Sea Ice	CICES5.1.2 360x300 (tripolar grid)	COCO4.9 360x256 (tripolar grid)	CICE5.1 320x384 with varying grid

NCAR-CESM2

The Community Earth System Model 2 (CESM2) from the National Center for Atmospheric Research (NCAR) was released in 2018 (Danabasoglu et al., 2019) with the components shown in Table 1. The choice of this model has been made as it is one of the best models for the representation of ENSO characteristics and its effects on the global climate (Capotondi et al., 2020). It incorporates land ice and biochemical processes, making it a very complete model compared to the other two used in this study.

2.4 Methods

2.4.1 Detrending climate data for short-term variability analysis

As we are interested in understanding processes related to short-term internal variability of the climate system, we remove the long-term trend to climate change using a 20-year moving average. This technique removes trends due to climate change,

and alleviates other fluctuations on a multi-decadal time scale. If a smaller window period was taken, the average would have been too influenced by single-year extremes. The last (and first) 10 years of the data are deducted from the 20-year average of 2003-2023 (and 20 first years), which can create a slight difference depending on the strength of the climate change signal. We calculate anomalies relative to monthly means and when necessary, data is seasonally averaged in winter (JJA), spring (SON), summer (DJF), autumn (MAM), or over the monsoon period (NDJFM).

2.4.2 Definition of the Australian Monsoon region and related areas

The AUM affects the tropical regions of Australia, however, there is no unique definition in the literature of what characterizes the monsoon area. We define a region affected by the monsoon as an area where there is a seasonal reversing of the major wind system (Krishnamurti et al., 2023). The monsoonal wind bringing moisture to NA comes mainly from southern Indonesia (Figure 2.2; see SIndo box) with a strong correlation between wind over southern Indonesia and precipitation over NA (Figure A4). The region of strong correlation delimited in Figure A4 is used in this study as the area affected by the AUM. This area also corresponds to the region described in previous research (Heidemann et al., 2023; Sekizawa et al., 2023; Yu and Notaro, 2020). However, due to varying grid resolution in the models and the reanalysis, this area was adjusted to fixed longitudes and latitudes that correspond best to the previous research and the correlation observed between wind and precipitation. The region chosen is the Australian land between 11 to 23° S and 122 to 149° E (Figure 2.2). Consequently, it was decided to separate the IMC into three distinct zones (Figure 2.2). One of those areas is the AUM region, with the dimension given above. The others are Southern Indonesia (SIndo, 10-14° S, 106-123° E) and West of Australia (WoA, 15-28° S, 90-100° E).

2.4.3 ENSO index and the definition of multi-year La Niña events

We used the ONI from A. T. Huang et al. (2024). The index was calculated back to 1900 using the ERSSTv.5 data, following the instructions from NOAA available at: origin.cpc.ncep.noaa.gov/products/analysis_monitoring/ensostuff/ONI_v5.php. Nine multi-year La Niña have been observed since 1940, with double events in 1954-56, 1970-72, 1983-85, 2007-09, 2010-12, 2016-18, and triple events in 1973-76, 1998-2001, and 2020-2023 (A. T. Huang et al., 2024). In addition, two other triple La Niña have been identified in (A. T. Huang et al., 2024) dating back to 1900: one event between 1907 and 1910, and another one between 1914 and 1917. To be considered a La Niña (El Niño) event, the ONI must be lower (higher) than -0.5 °C (0.5 °C) for at least five consecutive months; this threshold is approximately equivalent to $\frac{1}{2}\sigma$. One of the main challenges in the representation of ENSO by the CMIP6 models is the amplitude of this phenomenon. Each model has a different amplitude of ENSO which can have important repercussions on the representation of the real climate. Therefore, to minimize the inner model amplitude, and to be able to clearly compare the models and the reanalysis, it has been decided to use a standardized ONI.

The observed $|0.5|$ °C threshold cannot be taken for the models, as the ONI's standard deviation varies with each model (Figure A3). The NCAR-CESM2 has the biggest standard deviation with $\frac{1}{2}\sigma$ at 0.54°C, MIROC6 is at 0.47°C and ACCESS-CM2 at 0.42°C. To avoid considering single La Niña overlapping over two years as

multi-year events, at least one month of the La Niña usual peak (NDJFM) must be below -$\frac{1}{2}\sigma$. Therefore, a double-year La Niña will usually start at the end of year one and end at the beginning of year three. It will overlap three different years but only have two peaks. Multi-year La Niña is not considered as multiple years of constant La Niña but rather consecutive years where La Niña has developed.

2.5 Results

2.5.1 Internal monsoonal circulation and its intensification

Our first goal is to examine the IMC during La Niña years. To do that, we use different indicators in the three key regions shown in Figure 2.2. It is expected that in an intensified IMC (Figure 2.2), higher wind speed, and higher evaporation should stand out on the whole IMC area (Figure 2.2), as well as higher precipitation and higher soil moisture above the AUM region.

The relationship between precipitation in the AUM region and IMC can be seen in Figure 2.3. This figure shows an internal intensification of the monsoon with high soil moisture and evaporation in the AUM region, high wind speed, and evaporation over the Indian Ocean. More specifically, rainfall in NA shows a strong correlation with underlying soil moisture (coefficient of 0.9, Figure 2.3 f)) and evaporation (correlation of 0.89, Figure 2.3 c)). NA rainfall during the monsoon is also significantly correlated with evaporation and winds in Sindo and WoA (Figure 2.3 a), b), d), e)). This is consistent with the findings of Sekizawa et al. (2023) which describes an enhanced monsoonal system linked with soil moisture and evaporation in the eastern Indian Ocean. As expected, the correlation diminishes for the wind and the evaporation as we go further from the AUM region, with the lowest (yet significant) correlation seen in comparison with WoA. Third-year La Niña seems also susceptible to this circulation, with some specific characteristics. Indeed, even though it is challenging to come to any conclusion with three events, abnormally high soil moisture and evaporation are observed over the AUM region (Figure 2.3).

Figure 2.4 presents the precipitation and soil moisture in the AUM region averaged over the entire period and during multi-year La Niña events, alongside the average values and the ONI for these events. Each year of the multi-year events precipitation and soil moisture are more intense than the climatology. However, we can see that the first year has a strong peak in January and the third year sees intense rainfall between December and February. We can also note an important rainfall accumulation in the premises of the third monsoon. This could also play a role in the higher than expected soil moisture and evaporation found in the third year of La Niña (Figure 2.3 c), f)).

The evaporation enhancement is a consequence of high soil moisture and high rainfall in the AUM region rather than a temperature increase, as the temperature is abnormally low during the third year of La Niña in the AUM region (Figure 2.5 c)). Wind speed and consequently evaporation increases over Southern Indonesia and the Indian Ocean in the first year of La Niña (Figure 2.3 a), d)). These features are

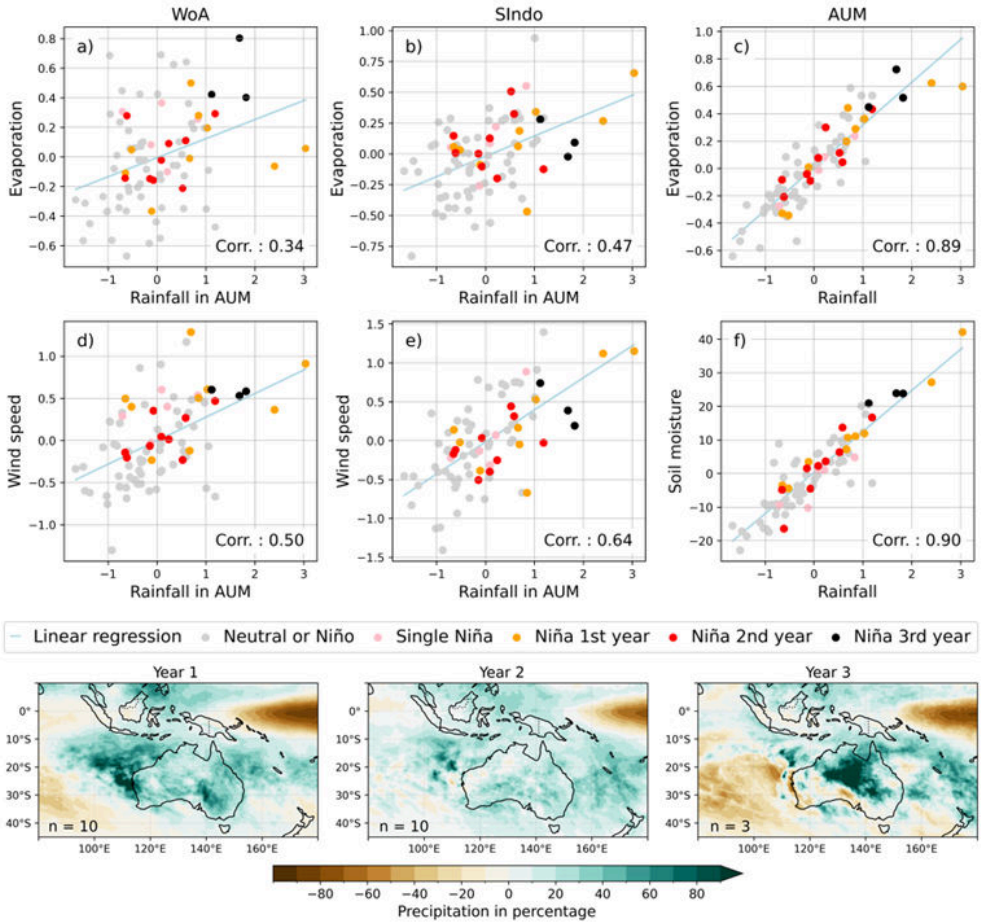

Figure 2.3: On the top row, the relationship between rainfall in mm/day in the Australian monsoon and evaporation in mm/day in a) West of Australia (WoA), b) South Indonesia (SIndo), and c) Australian monsoon (AUM) regions. In the middle row, the wind speed in m/s in d) WoA e) SIndo; and, f) soil moisture in mm of water per m of soil in AUM. Regions are identified by green boxes in 2.2. All of them have been detrended by a 20-year moving average and are represented during the monsoonal period NDJFM. On the bottom row is the rainfall anomaly in percentage in NDJFM during the first year, h) second year, and i) third year of multi-year La Niña.

amplified in the third year of triple La Niña over WoA, including a strong equatorward displacement of moisture (Figure 2.5 d)). This moisture is then brought back over NA via the IMC (Figure 2.5 d)). In the SIndo region, the circulation is stronger than the mean state during the third-year La Niña (Figure 2.5 c) d)). However, linked to the amount of rainfall produced in the AUM region during the third-year La Niña, the circulation is not stronger than what the linear regression curve would suggest. It is seen in Figure 2.3 b), e) with wind speed and evaporation of third-year La Niña close to the linear regression curve.

One possible explanation for the IMC being stronger than expected during the third year of La Niña in the AUM region and WoA, but not in the SIndo, is the influence of higher soil moisture. Increased soil moisture from preceding rainfall events before the monsoon could provide additional energy, facilitating the onset of the IMC. This would create a more intense circulation during the monsoon and the whole circulation would be enhanced. However, this circulation slightly weakens in the northern

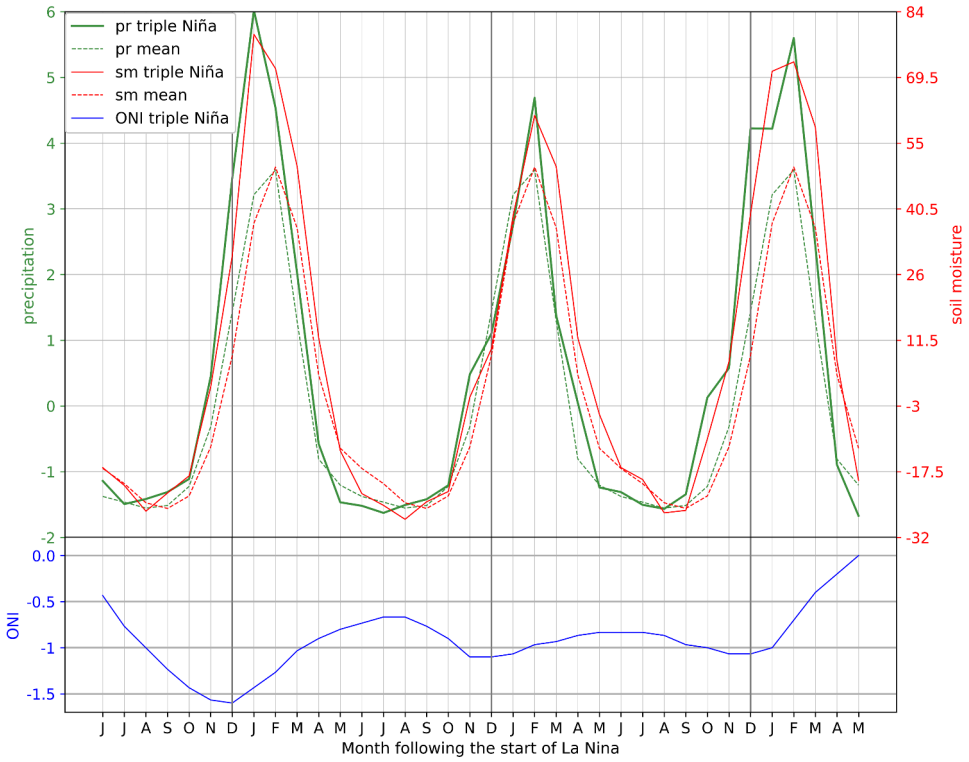

Figure 2.4: Rainfall, and soil moisture during the three triple year La Niña in the AUM region and the mean rainfall and soil moisture in the same region in dashed with ERA5 and AWRA-L. On the bottom, the ONI during the triple year La Niña.

part compared to what the linear regression suggests (Figure 2.3 b), e)). It is possibly because the initial fuelling is not reinforced enough in this area due to lower SST in SIndo (Figure 2.5 c)).

During the three third-year La Niña events in ERA-5, precipitation tends to be notably stronger. The abnormally high spike during the first year of La Niña can be explained by the very low values of ONI leading to high precipitation, especially in 1973 with record-breaking rainfall (Figure A1). The increased monsoon rainfall in the first year of La Niña typically initiates in November, exhibiting a peak in January (Figure 2.4).

During the third year of La Niña in NA, higher precipitation in October is observed (Figure 2.4), suggesting an earlier monsoon onset. This earlier monsoon onset could increase soil moisture one season ahead of the monsoon peak. This could trigger an IMC intensification, which is in line with Sekizawa et al. (2023) findings. The earlier rainfall could be due to the length of the La Niña episode or the low ONI during the austral winter between the second and third La Niña event. Indeed, usually La Niña events peak during austral summer as observed in the first year (Figure 2.4). However, between the second and third events, the ONI stays around -1° C, which could also have some repercussions on rainfall in NA before the start of the monsoon. In the third year of a triple-year La Niña, the ONI quickly returns to neutral, with ENSO conditions becoming neutral before March. The strength of La Niña in the

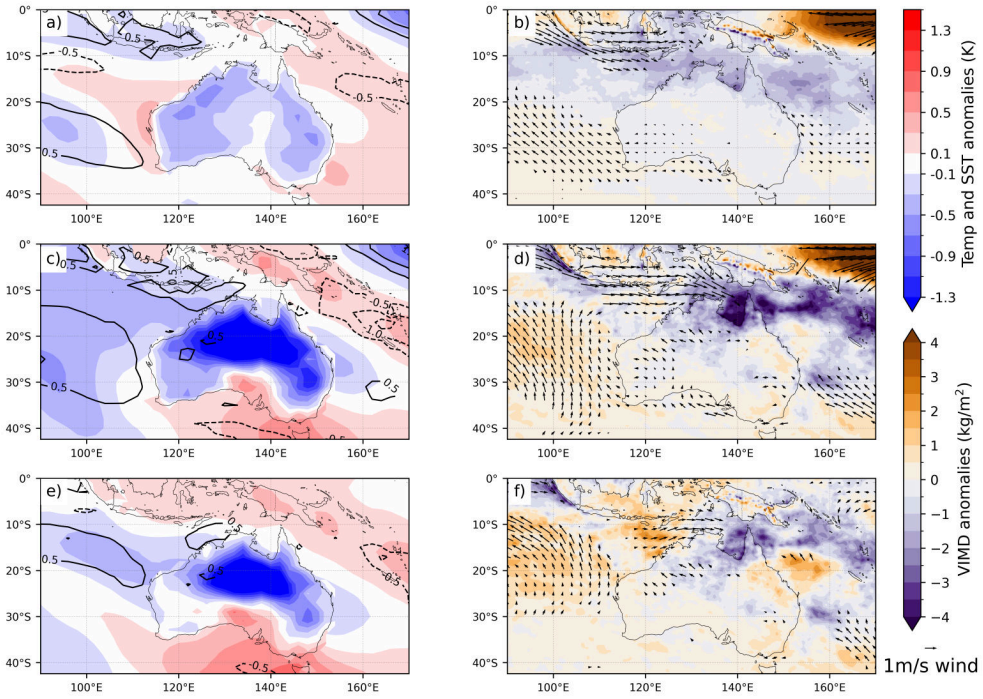

Figure 2.5: The left row represents the anomalies of wind speed (in contours), SST, or air temperature when on land, during the monsoon (NDJFM). The right row represents wind anomalies (in arrows) and Vertically Integrated Moisture Divergence (VIMD). a) and b) use the anomalies during the first year of La Niña. c) and d) use the anomalies during the third year of La Niña. e) and f) represent the difference between the third year and the first year of La Niña (Year 3 - Year 1).

third year is weaker compared to the first and second year (Figure 2.4), which suggests a decoupling of the monsoonal rainfall with ENSO. Furthermore, soil moisture seems to go nearly back to average at the end of winter (June-September) despite enhanced precipitation in the previous years. During the third year La Niña, a rapid increase in precipitation earlier in the calendar year acts to enhance soil moisture in spring, which in turn enhances precipitation at the peak of the monsoon (Figure 2.4).

A more visual approach to differences between first-year and third-year La Niña is shown in Figure 2.5. During the third year, the temperature of the Indian Ocean as well as temperatures over NA are well below the average for this season. The temperature anomaly over Australia is strongly negative. The low continental temperatures above NA might be explained by the earlier onset of the monsoon, as well as an already high soil moisture. Higher soil moisture can enhance latent heat flux to the atmosphere which increases evaporation of water content of the soil; thus causing anomalous land surface cooling (Hope and Watterson, 2018). Furthermore, strong northwesterly winds linked to the monsoon low-pressure system during the third year, bring moisture from the eastern Indian Ocean to the Northern Territory and northern Queensland. We can note that Figure 2.5 shows all first-year La Niña, however, Figure 2.4 considers only the three years of triple La Niña.

2.5.2 Models' representation of multi-year La Niña

The models included in this study all had difficulties adequately reproducing the frequency and/or the variations of multi-year La Niña events. Indeed, the ERSSTv5 reanalysis shows a frequency of triple La Niña events of around 2.9 events per century (5 events since 1854; see Methods section 2.4.3)). In the models, this frequency varies considerably with MIROC6 having 3.6 events per century (29 events in 800 years), 1.3 events per century for NCAR-CESM2 (15 events in 1200 years), and ACCESS-CM2 having none. It is well known that the ACCESS-CM2 has a marked biennial ENSO (Bi et al., 2022; Rashid et al., 2022). The ACCESS-CM2 model does not catch triple-year La Niñas due to its marked biennial ENSO. It is, therefore, not surprising that it does not simulate multi-year La Niñas. Considering a lower threshold of $-\frac{1}{4}\sigma$ for the ACCESS-CM2 identifies 8 events in 500 years (1.6 events per century). This will be used as an indication of weak multi-year La Niña.

The ONI composite of multi-year La Niñas of the models is shown in Figure 2.6. All models have different amplitudes and evolution when reproducing the triple La Niña. MIROC6 simulates a weaker first-year La Niña and a stronger second-year. This model recreates the peak of La Niña during austral spring (SON) which could cause a biased simulation of monsoonal rainfall (Figure 2.6). Then, the triple-event simulated by the NCAR-CESM2 is essentially a La Niña slowly fading away year by year, peaking in December in all three years. Finally, triple-year La Niñas in the ACCESS-CM2 model has a weak second year and go back to a neutral state between the second and third year due to its biennial ENSO (Rashid et al., 2022). The representation of the ONI is an important feature of models. Indeed, if the peak of ENSO is too early, as seen with MIROC6 (Figure 2.6), the impact of ENSO will also be shifted. If ENSO is generally too strong, with higher deviation as seen with MIROC6 and NCAR-CESM2, there is a risk of having a stronger impact of ENSO than in real conditions.

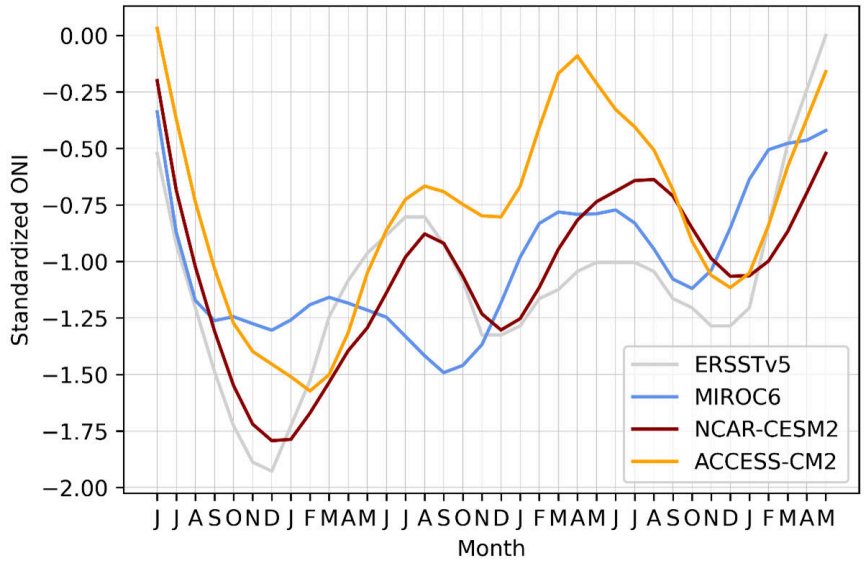

Figure 2.6: Standardized ONI evolution during triple-year La Niña

2.5.3 The La Niña effect on the AUM

This section examines the modeled AUM during triple La Niña. The ERA-5 reanalysis shows third-year rainfall enhancement has two main characteristics. The first is an unusually important precipitation early in the season, as soon as September-October (SO). The second is enhanced rainfall during austral summer. It is therefore important to analyze separately those two periods, before the monsoon, in SO, and during the monsoon (NDJFM), to establish whether the IMC and/or its intensification of rainfall can be simulated.

In the premises of the AUM, in early spring (Figure 2.7), we can identify the contour of a low-pressure system associated with the build-up of the AUM with ERA-5 in year 3 in northwestern Australia. This circulation is linked with the warm moist north-westerly monsoon low pressure suggested by Figure 2.2 and visible in Figure 2.5 d), which depicts an IMC set earlier during multi-year La Niña. This early onset of the AUM can be identified in the NCAR-CESM2 in years 2 and 3, with year 2 having extreme precipitation in early spring. MIROC6 shows a small rainfall intensification in the same region in year 2 during SO. The ACCESS-CM2 model does not reproduce the early monsoonal rainfall as expected, due to its low ability to reproduce multi-year La Niña events.

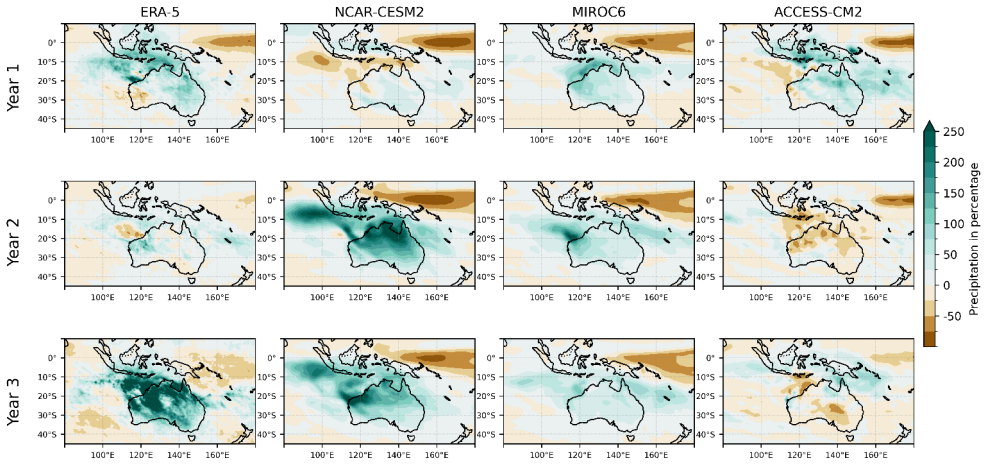

Figure 2.7: Rainfall in early spring, September and October, in percentage difference compared to the mean during the first, second, and third year with ERA-5, NCAR-CESM2, MIROC6, and ACCESS-CM2.

The intensification of the AUM in year 3 is visible in the ERA-5 reanalysis (Figure 2.8), especially in the center of NA. None of the chosen models represent the third-year AUM rainfall enhancement to the same extent and intensity as the observed. This could be caused, among other things, by the variation of the triple-year ONI between the models and the reanalysis. While the NCAR-CESM2 model does not show an enhancement of the third-year La Niña rainfall, it successfully simulates an intensification of the AUM after the intense SO rainfall in the second year. MIROC6 somewhat reflects increased precipitation in the second year but not in the third. Additionally, it portrays a higher percentage of rainfall in spring but does not properly show the monsoonal circulation seen in ERA-5. The ACCESS-CM2 model does not seem to be influenced by multi-year La Niña. Even though this model represents ENSO's westward extension well, it fails to depict the rainfall increase during

the AUM. The other two models have an excessive westward extension of the precipitation (Figure 2.8), which is a known bias of the CMIP6 models (Jiang et al., 2021).

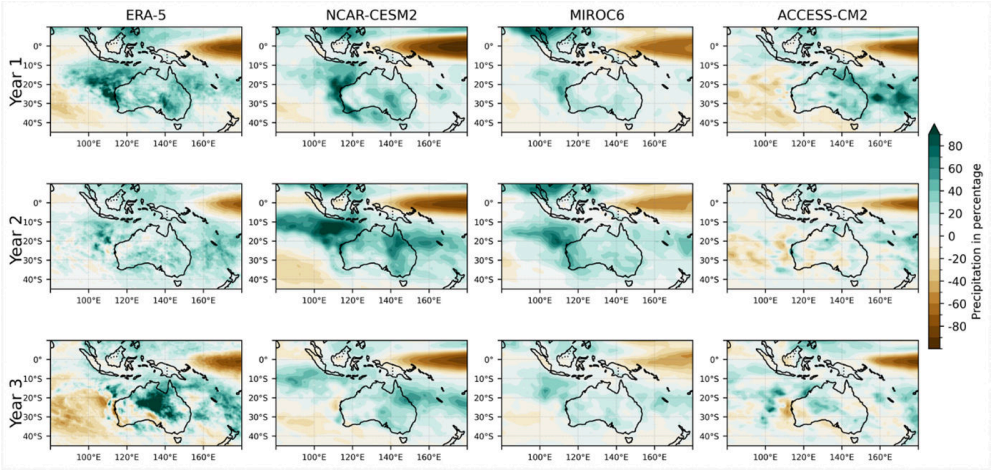

Figure 2.8: Rainfall in monsoon season (NDJFM) in percentage difference compared to the mean during the first, second, and third year with ERA-5, NCAR-CESM2, MIROC6, and ACCESS-CM2.

As described above, an increase in precipitation is visible in the second year with NCAR-CESM2 and MIROC6. The shape of this enhancement seems closer to the year 1 ERA-5 rainfall anomaly than the year 3. We will still try to understand this second-year enhancement, as the strength of La Niña weakens (Figure 2.6) but exhibits stronger precipitation, a pattern similar to the third-year rainfall increase observed in ERA-5.

2.5.4 Triple-year La Niña characteristic of the NCAR-CESM2

This part of the study focuses on the NCAR-CESM2 characteristics of the triple-year La Niña (Figure 2.9) as it best represents the AUM patterns. There is a difference in the magnitude of the ONI between ERA5 (Figure 2.4) and the NCAR-CESM2 (Figure 2.9), and thus it has been standardized to facilitate the comparison with ERA5.

The soil moisture in NCAR-CESM2 is accumulated in-depth (Lawrence et al., 2019). Therefore, its values are bigger than AWRA-L v.6 reanalysis where only the water in the first meter of soil is taken into account. Therefore, we tend to see a stronger soil moisture enhancement over the years in the model. It also explains the shift in soil moisture's peak of one or two months between Figure 2.4 and Figure 2.9, as the water accumulates deeper in the soil in the NCAR-CESM2 model. The monthly precipitation reveals a similar effect to that observed in the reanalysis data. Indeed, earlier rainfall is discernible during the second and third years of La Niña events. The enhanced precipitation in the third year seems to indicate a stronger soil moisture component in the setting of an early IMC.

The soil moisture in deep layers can play a role in rainfall enhancement, as seen with ERA-5. Indeed, as the deep layers are already saturated before the start of the AUM, the water cannot go deep and the surface is saturated faster. As the surface is saturated, latent heat production is prioritized, which lowers the surface temperature

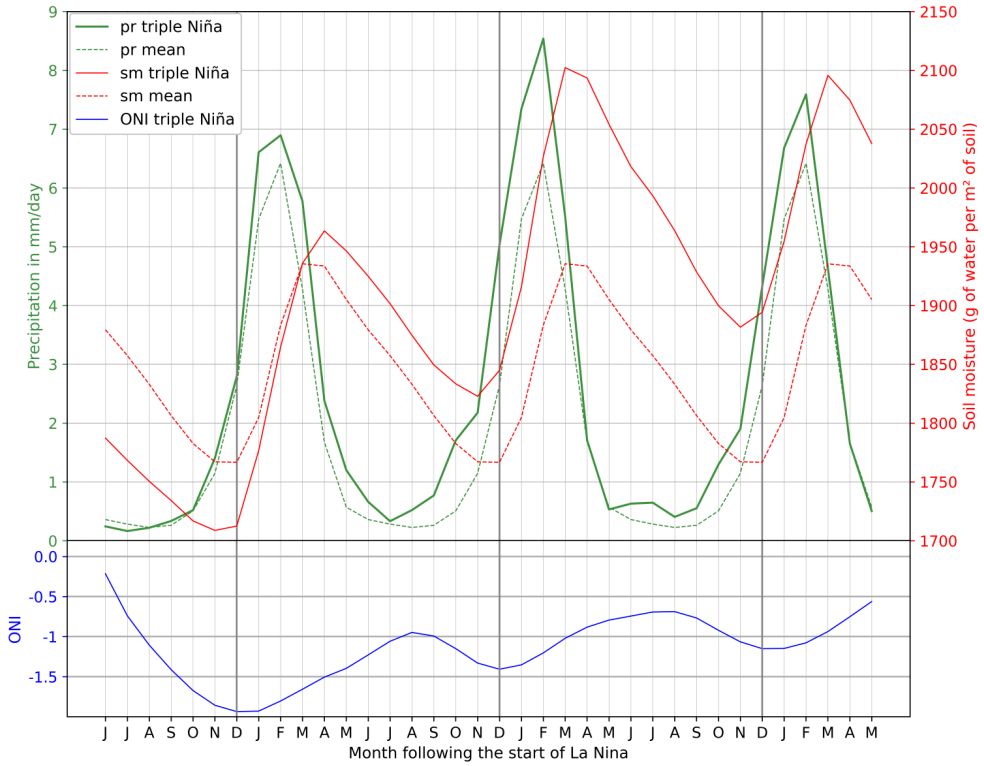

Figure 2.9: Rainfall, and soil moisture during triple year La Niña in the AUM region and the mean rainfall and soil moisture in the same region in dashed for the NCAR-CESM2 model. On the bottom, the ONI during the triple year La Niña.

and favors precipitation. This mechanism would not explain the earlier onset of the monsoon but could explain the strength of the monsoon in the third year of La Niña.

2.6 Discussion and Conclusion

The study aimed to understand better what creates intense precipitation in the third year of multi-year La Niña, despite La Niña weakening. In a first step, we identified an intensified IMC as described by Sekizawa et al. (2023). Third-year La Niña appears to have higher soil moisture, evaporation, and precipitation over NA (Figure 2.3 c), f)), and higher wind speed and evaporation in the Indian Ocean, to the West of Australia (Figure 2.3 a), d)). Together with the earlier precipitation in early spring, an earlier and intensified IMC is an important feature of the third year of La Niña (Figure 2.7). This IMC is strengthened by high soil moisture in NA. The early onset of the intensified IMC seems to be linked with La Niña between the second and third monsoon. Increased precipitation occurs in early spring, thus intensifying soil moisture, which in turn enhances monsoonal rainfall in NDJFM.

With the analysis of preindustrial control run in three CMIP6 models, we saw that multi-year rainfall enhancement is also visible, as well as an earlier IMC, even with lower ONI in the second or third year of La Niña. Out of the three models tested, the NCAR-CESM2 represented the IMC as well as rainfall intensification during multi-year la Niña. The MIROC6 has also shown a multi-year La Niña rainfall increase but the rainfall patterns and the La Niña peak are less realistic. The ACCESS-CM2 model

failed to recreate triple-year La Niña, compromising the rainfall analysis. Looking more into the details of the triple-year La Niña of the NCAR-CESM2, it appears that earlier rainfall seems to increase soil moisture in early spring and leads to increased rainfall recycling and stronger monsoon in NDJFM. Together with higher ONI during austral winter, the CESM2 seems to have a strong inter-monsoonal rainfall enhancement. This result is consistent with the findings by Sharmila and Hendon (2020) who showed that northwestern Australia is sensitive to rainfall-wind-evaporation feedback. Here we show that the feedback mechanism can extend to the entire northern and central regions of Australia, in the third year of La Niña.

The mechanisms involved in the extreme multiple-year La Niña are summarized in Figure 2.10. As seen with the reanalysis and the models, a low-pressure anomaly in northwestern (NW) Australia seems to be an important feature of this strong AUM. Different factors could explain these early AUM patterns, such as the La Niña development in late winter and spring, and ocean memory. This low pressure brings early rainfall over the AUM region. As the soil is wetter than usual due to an earlier season of above-average rainfall, it enhances evaporation and triggers an early onset of the monsoonal circulation. During the monsoon period, we see an internal positive feedback as described by Sekizawa et al. (2023) with an intensified monsoonal circulation triggering higher rainfall, leading to more soil moisture and therefore more evaporation, which intensifies the monsoonal circulation. The early precipitation, saturated soil, and premature onset of the monsoonal circulation help this positive feedback to get stronger. The mechanism described by Sekizawa et al. (2023) is, however, independent of ENSO. Here we show that this mechanism of self-sustaining monsoon can operate in the third year of multi-year La Niña as the Central Pacific SST weakens, allowing for it to act.

Given the limited dataset comprising only three triple-year La Niña events, it is reasonable to anticipate highly inconsistent outcomes between the models and the reanalysis data. The biggest flaw of the model comparison is possibly the differences in ONI between the model and the reanalysis, leading to a difference in the response of the AUM. Furthermore, this study focuses on the impact of ENSO and soil moisture, but there are multiple factors influencing the duration and the magnitude of the AUM, such as the Pacific multi-decadal variability (Heidemann et al., 2022) or the Ningaloo Niño/Niña events (Heidemann et al., 2023; Zheng et al., 2020). What is probably seen during the triple-year La Niña is a mix of both inter- and intra-monsoonal rainfall enhancement, with some external factors, leading to extreme precipitation. One way of delving deeper into the subject would be to investigate the results of a model that can reproduce a more realistic, and an earlier La Niña peak to explore how rainfall preceding austral summer would affect the AUM. Future work could also use numerical experiments with idealized SST forcing representation of observed multi-year La Niña to understand how the amplitude and timing affect soil moisture over NA and lead to enhanced monsoon.

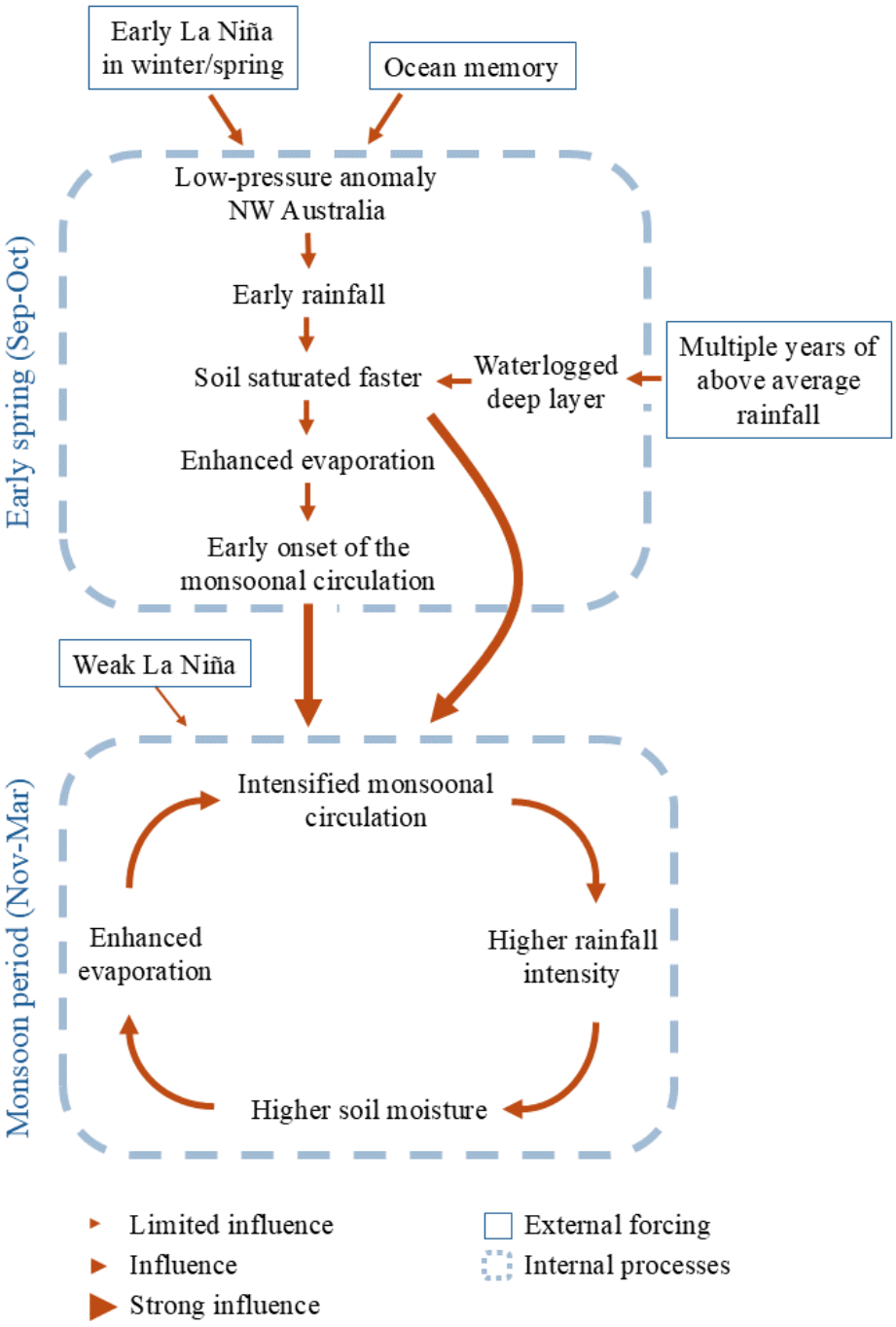

Figure 2.10: Schematic of the mechanisms during the third-year La Niña. The situation during early-spring (September-October) in the top square and during the monsoon period (November to March) in the bottom square.

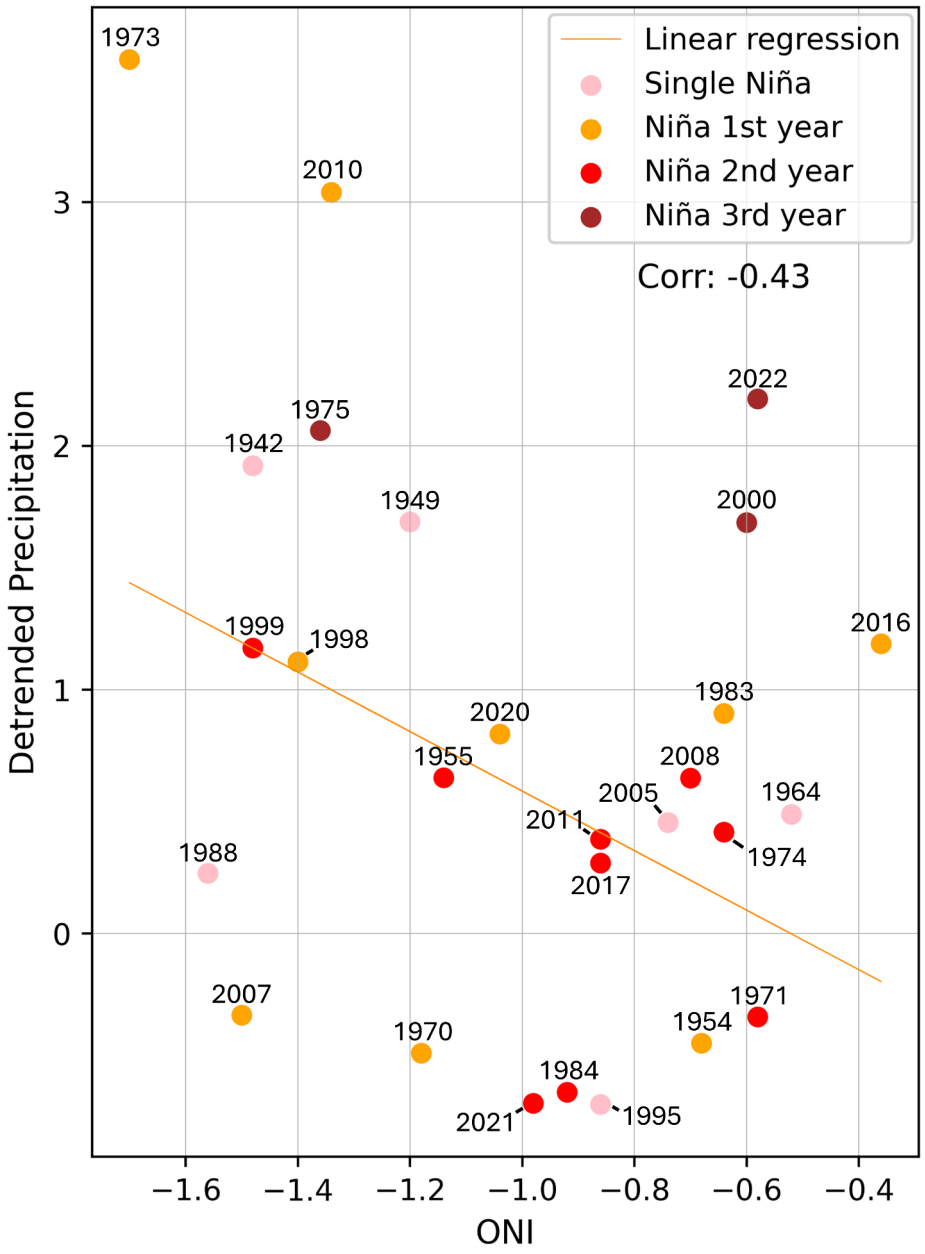

A1 Scatter plot of the ONI in NDJFM and the detrended precipitation (in mm/day compared to the 20-year average) in the AUM region in NDJFM. As the AUM straddles two years, here is written only the first year.

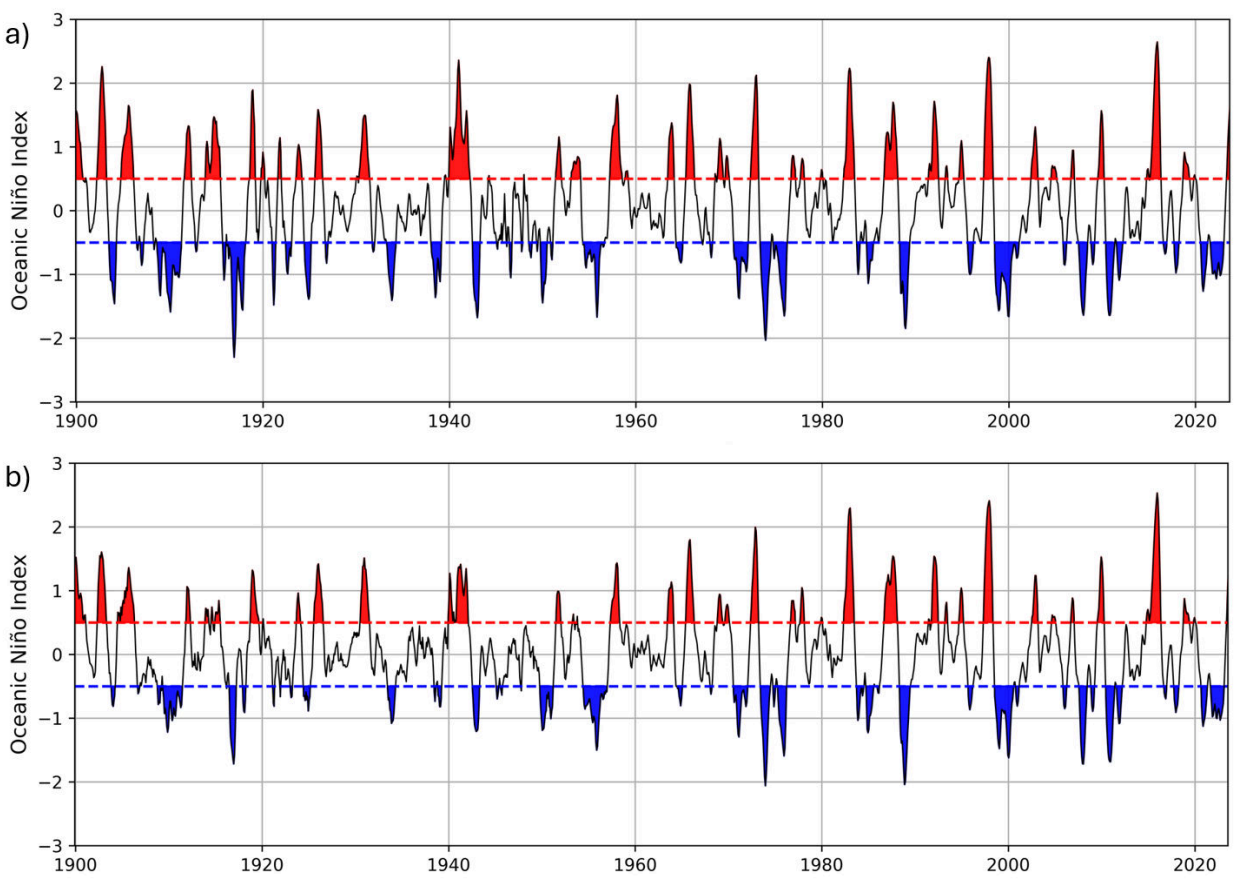

A2 ONI since 1900 with a) ERSSTv5 and b) HadISST.

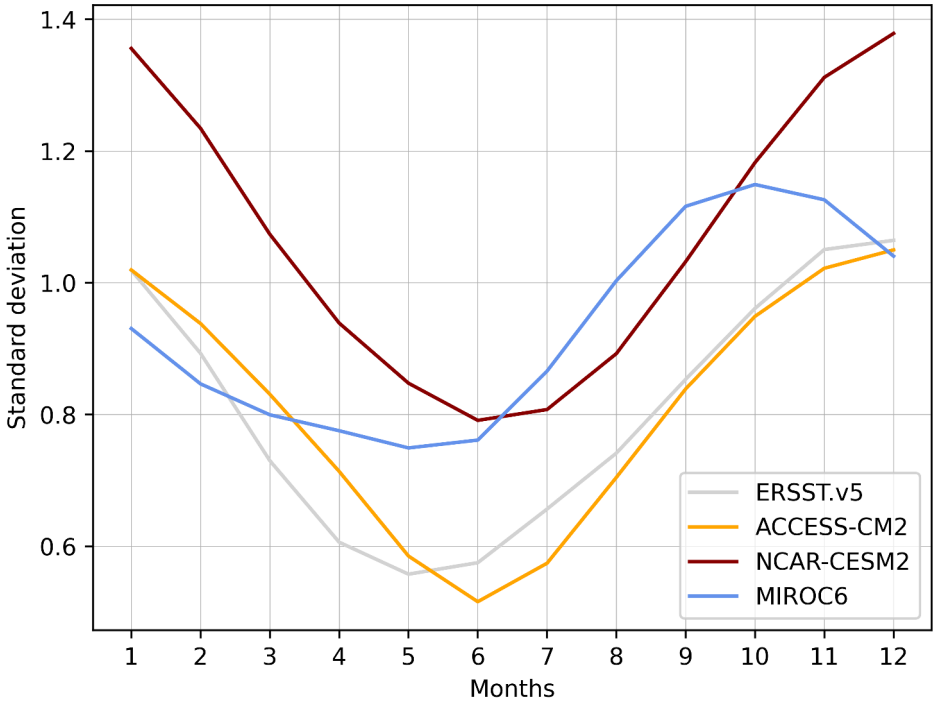

A3 Standard deviation of the monthly SST in the Ninño3.4 region with different models and with the ERSST.v5.

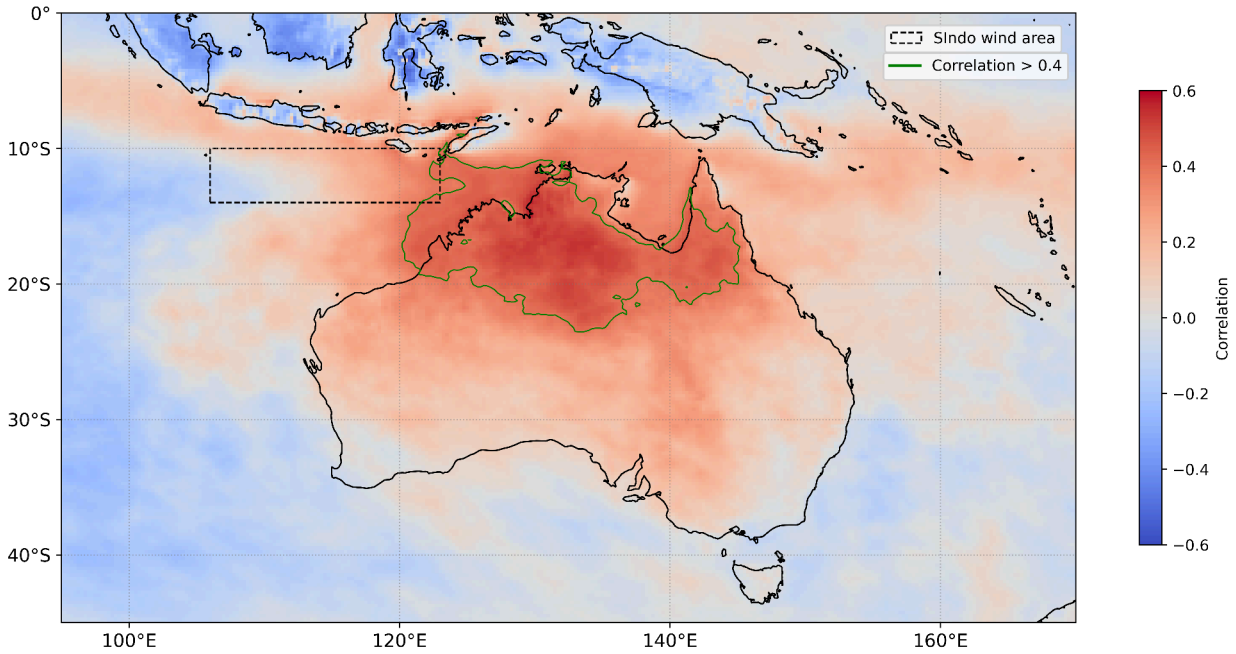

A4 Correlation between wind in SIndo, in dashed, and precipitation in NDJFM. Correlation over 0.4 inside the green contour.

3 Future prospect

This thesis aims to investigate the mechanisms driving increased AUM rainfall in the third year of a triple La Niña event. The findings suggest that soil moisture alone is unlikely to explain the enhanced rainfall observed. Another factor contributing to the early rainfall is likely the earlier peak of the La Niña during the winter and spring preceding the third year of La Niña, which triggers an earlier onset of the monsoon.

The ENSO typically peaks in the austral summer. However, this peak can shift to earlier or later in the year. This shifting of the peak can have significant implications for different regions. The La Niña peak shifting in early spring instead of mid-summer seemed to be a key feature of the rainfall enhancement of the triple-year La Niña. The consequences of this unusual early La Niña have not yet been thoroughly studied but appear to be significant, particularly in NA.

To delve into the subject, we plan to investigate the impact of an early La Niña peak and retreat on the AUM using a suite of climate models available from the CMIP6. Finally, we also plan to design an idealized experiment using the NCAR-CESM1.2 model with an atmospheric-only component and fixed SST. The SST will be tuned in the tropical Pacific Ocean to simulate an early La Niña peak and analyze its influence over Australia and surrounding regions. The adjusted SST corresponds to the average of all La Niña events since 1940, with negative anomalies applied over the tropical Pacific Ocean. Simulations will be conducted from January of year 0 through April of year 3, with one set featuring the La Niña peak in austral summer, and another featuring a peak in austral spring. Each scenario will include 10 ensemble members. Additionally, a 30-year control run without external forcing will be performed to establish the climatology.

By doing this we would like to find out if La Niña's peaks can influence the Australian summer, especially the AUM. This research aims to deepen our understanding of La Niña's overall impact on the Australian climate and improve forecasting accuracy.

4 Acknowledgments

I would like to thank my advisor Ass. Prof. Andréa S. Taschetto who gave me this amazing opportunity to become part of her research team at the UNSW. Her support, dedication, and the time she invested weekly in guiding me through this work have been invaluable. I am deeply grateful for her mentorship and for believing in my potential.

My sincere thanks also go to Prof. Stefan Brönnimann, who graciously agreed to supervise this project despite having no formal obligation or affiliation. His willingness to support me has been crucial to the success of this Thesis.

I am profoundly thankful to my family, without whom this experience would not have been possible. They supported me throughout this journey, even when they did not always agree with my choices. Their encouragement has been a constant source of strength for me.

I would also like to acknowledge my beloved girlfriend, Zoé, my favorite human. Without hesitation, she accepted the challenge of being apart for nearly a year. It was undoubtedly difficult at times, but her constant support, endless encouragement, and presence, even from thousands of kilometers away, meant the world to me. I couldn't have done this without her.

A huge thanks to Guillaume (giomm.ch) who provided me with some much needed help and experience in the creation of different schematics.
A heartfelt thank you to my dear friends, Valentin and Loïc, who were always there when I needed someone to talk to. Their friendship and understanding helped me navigate the ups and downs of this journey.
Lastly, I would like to extend my gratitude to Melina Lisanne for her much-needed assistance with all the IT-related challenges I encountered. Your help was indispensable, and I am truly appreciative.

5 Data availability statement

The gridded monthly reanalysis data from ERA5, available since 1940, can be accessed on their official website at cds.climate.copernicus.eu/datasets/reanalysis-era5-single-levels?tab=download (Hersbach et al., 2023). The NOAA ERSSTv.5 dataset (B. Huang et al., 2017) is publicly available at
https://psl.noaa.gov/data/gridded/data.noaa.ersst.v5.htm.
The AWRA-L model data (Frost et al., 2018) can be obtained through the AWRA CMS GitHub repository (https://github.com/awracms/awra_cms). Finally, the pre-industrial control run datasets of the climate models (Danabasoglu et al., 2019; Dix et al., 2019; Tatebe and Watanabe, 2018) were retrieved from the Australian National Computational Infrastructure (NCI) and are available on the NCI's website (https://my.nci.org.au/mancini/project/fs38). These datasets are also freely accessible via the Earth System Grid Federation Climate Data Gateway at:
https://aims2.llnl.gov/search/?project=CMIP6.

Bibliography

Ashok, K., Behera, S. K., Rao, S. A., Weng, H., & Yamagata, T. (2007). El Niño Modoki and its possible teleconnection. *Journal of Geophysical Research: Oceans*, *112*(C11). https://doi.org/10.1029/2006JC003798

Australian Bureau of Meteorology. (n.d.-a). Australia's official weather forecasts & weather radar - Bureau of Meteorology. Retrieved July 16, 2024, from http://www.bom.gov.au/?ref=logo

Australian Bureau of Meteorology. (n.d.-b). The Australian Monsoon. Retrieved January 14, 2024, from http://www.bom.gov.au/climate/about/?bookmark=monsoon

Australian Bureau of Meteorology. (n.d.-c). The Madden-Julian Oscillation. Retrieved January 24, 2024, from http://www.bom.gov.au/climate/about/?bookmark=mjo

Australian Bureau of Meteorology. (n.d.-d). Northern rainfall onset outlook. Retrieved January 14, 2024, from http://www.bom.gov.au/climate/rainfall-onset/#tabs=About-the-rainfall-onset

Berg, A., Lintner, B., Findell, K., & Giannini, A. (2017). Soil Moisture Influence on Seasonality and Large-Scale Circulation in Simulations of the West African Monsoon. *Journal of Climate*, *30*(7), 2295–2317. https://doi.org/10.1175/JCLI-D-15-0877.1

Berry, G. J., Reeder, M. J., & Jakob, C. (2012). Coherent synoptic disturbances in the australian monsoon. *Journal of Climate*, *25*(24), 8409–8421.

Berry, G. J., & Reeder, M. J. (2016). The dynamics of australian monsoon bursts. *Journal of the Atmospheric Sciences*, *73*, 55–69. https://api.semanticscholar.org/CorpusID:120119472

Bi, D., Wang, G., Cai, W., Santoso, A., Sullivan, A., Ng, B., & Jia, F. (2022). Improved simulation of enso variability through feedback from the equatorial atlantic in a pacemaker experiment. *Geophysical Research Letters*, *49*(2), e2021GL096887.

Bui, H. X., Li, Y.-X., Sherwood, S. C., Reid, K. J., & Dommenget, D. (2023). Assessing the soil moisture-precipitation feedback in Australia: CYGNSS observations. *Environmental Research Letters*, *19*(1), 014055. https://doi.org/10.1088/1748-9326/ad15b7

Cai, W., Rensch, P. v., Cowan, T., & Hendon, H. H. (2012). An Asymmetry in the IOD and ENSO Teleconnection Pathway and Its Impact on Australian Climate. https://doi.org/10.1175/JCLI-D-11-00501.1

Cai, W., Santoso, A., Collins, M., Dewitte, B., Karamperidou, C., Kug, J.-S., Lengaigne, M., McPhaden, M. J., Stuecker, M. F., Taschetto, A. S., Timmermann, A., Wu, L., Yeh, S.-W., Wang, G., Ng, B., Jia, F., Yang, Y., Ying, J., Zheng, X.-T., … Zhong, W. (2021). Changing El Niño–Southern Oscillation in a warming climate. *Nature Reviews Earth & Environment*, *2*(9), 628–644. https://doi.org/10.1038/s43017-021-00199-z

Capotondi, A., Deser, C., Phillips, A. S., Okumura, Y., & Larson, S. M. (2020). ENSO and Pacific Decadal Variability in the Community Earth System Model Version 2 [_eprint: https://onlinelibrary.wiley.com/doi/pdf/10.1029/2019MS002022]. *Journal of Advances in Modeling Earth Systems*, *12*(12), e2019MS002022. https://doi.org/10.1029/2019MS002022
e2019MS002022 2019MS002022.

Chambers, D., Tapley, B., & Stewart, R. (1999). Anomalous warming in the indian ocean coincident with el niño. *Journal of Geophysical Research: Oceans*, *104*(C2), 3035–3047.

Chiew, F. H. S., Piechota, T. C., Dracup, J. A., & McMahon, T. A. (1998). El Nino / Southern Oscillation and Australian rainfall, streamflow and drought: Links and potential for forecasting. *Journal of Hydrology*, *204*(1), 138–149. https://doi.org/10.1016/S0022-1694(97)00121-2

Chung, C., Boschat, G., Taschetto, A., Narsey, S., McGregor, S., Santoso, A., & Delage, F. (2023). Evaluation of seasonal teleconnections to remote drivers of australian rainfall in cmip5 and cmip6 models. *Journal of Southern Hemisphere Earth Systems Science*, *73*(3), 219–261.

Chung, C., & Power, S. (2017). The non-linear impact of El Niño, La Niña and the Southern Oscillation on seasonal and regional Australian precipitation. *Journal of Southern Hemisphere Earth System Science*, *67*, 25–45. https://doi.org/10.22499/3.6701.003

Danabasoglu, G., Lawrence, D., Lindsay, K., Lipscomb, W., & Strand, G. (2019). NCAR CESM2 model output prepared for CMIP6 CMIP piControl. https://doi.org/10.22033/ESGF/CMIP6.7733

Dey, R., Lewis, S. C., & Abram, N. J. (2019). Investigating observed northwest australian rainfall trends in coupled model intercomparison project phase 5 detection and attribution experiments. *International Journal of Climatology*, *39*(1), 112–127.

DiNezio, P. N., Deser, C., Karspeck, A., Yeager, S., Okumura, Y., Danabasoglu, G., Rosenbloom, N., Caron, J., & Meehl, G. A. (2017). A 2 Year Forecast for a 60–80% Chance of La Niña in 2017–2018. *Geophysical Research Letters*, *44*(22), 11, 624–11, 635. https://doi.org/10.1002/2017GL074904

Dix, M., Bi, D., Dobrohotoff, P., Fiedler, R., Harman, I., Law, R., Mackallah, C., Marsland, S., O'Farrell, S., Rashid, H., Srbinovsky, J., Sullivan, A., Trenham, C., Vohralik, P., Watterson, I., Williams, G., Woodhouse, M., Bodman, R., Dias, F. B., … Yang, R. (2019). CSIRO-ARCCSS ACCESS-CM2 model output prepared for CMIP6 CMIP piControl. https://doi.org/10.22033/ESGF/CMIP6.4311

Dommenget, D., Bayr, T., & Frauen, C. (2013). Analysis of the non-linearity in the pattern and time evolution of el niño southern oscillation. *Climate dynamics*, *40*, 2825–2847.

Douville, H., Conil, S., Tyteca, S., & Voldoire, A. (2007). Soil moisture memory and west african monsoon predictability: Artefact or reality? *Climate dynamics*, *28*(7), 723–742.

Eyring, V., Bony, S., Meehl, G. A., Senior, C. A., Stevens, B., Stouffer, R. J., & Taylor, K. E. (2016). Overview of the Coupled Model Intercomparison Project Phase 6 (CMIP6) experimental design and organization [Publisher: Copernicus GmbH]. *Geoscientific Model Development*, *9*(5), 1937–1958. https://doi.org/10.5194/gmd-9-1937-2016

Freund, M. B., Marshall, A. G., Wheeler, M. C., & Brown, J. N. (2021). Central Pacific El Niño as a Precursor to Summer Drought-Breaking Rainfall Over Southeastern Australia. *Geophysical Research Letters*, *48*(7), e2020GL091131. https://doi.org/10.1029/2020GL091131

Frost, A. J., Ramchurn, A., & Smith, A. (2018). *Technical Description of the Australian Water Resources Assessment Landscape model version 6* (tech. rep.). Bureau of Meteorology Technical Report. https://awo.bom.gov.au/assets/notes/publications/AWRALv6_Model_Description_Report.pdf

Gadgil, S. (2018). The monsoon system: Land–sea breeze or the ITCZ? *Journal of Earth System Science*, *127*(1), 1. https://doi.org/10.1007/s12040-017-0916-x

Geen, R., Bordoni, S., Battisti, D. S., & Hui, K. (2020). Monsoons, itczs, and the concept of the global monsoon. *Reviews of Geophysics*, *58*(4), e2020RG000700.

Geng, T., Jia, F., Cai, W., Wu, L., Gan, B., Jing, Z., Li, S., & McPhaden, M. J. (2023). Increased occurrences of consecutive la niña events under global warming. *Nature*, *619*(7971), 774–781.

Gillett, Z. E., Hendon, H. H., Arblaster, J. M., & Lin, H. (2023). Sensitivity of the southern hemisphere wintertime teleconnection to the location of enso heating. *Journal of Climate*, *36*(8), 2497–2514. https://doi.org/10.1175/JCLI-D-22-0159.1

Grose, M. R., Narsey, S., Delage, F., Dowdy, A. J., Bador, M., Boschat, G., Chung, C., Kajtar, J., Rauniyar, S., Freund, M., et al. (2020). Insights from CMIP6 for Australia's future climate. *Earth's Future*, *8*(5), e2019EF001469.

Ha, K.-J., Kim, B.-H., Chung, E.-S., Chan, J. C., & Chang, C.-P. (2020). Major factors of global and regional monsoon rainfall changes: Natural versus anthropogenic forcing. *Environmental Research Letters*, *15*(3), 034055. https://doi.org/10.1088/1748-9326/ab7767

Heidemann, H., Cowan, T., Henley, B. J., Ribbe, J., Freund, M., & Power, S. (2023). Variability and long-term change in Australian monsoon rainfall: A review. *WIREs Climate Change*, *14*(3), e823. https://doi.org/10.1002/wcc.823

Heidemann, H., Ribbe, J., Cowan, T., Henley, B. J., Pudmenzky, C., Stone, R., & Cobon, D. H. (2022). The Influence of Interannual and Decadal Indo-Pacific Sea Surface Temperature Variability on Australian Monsoon Rainfall. *Journal of Climate*, *35*(1), 425–444. https://doi.org/10.1175/JCLI-D-21-0264.1

Hendon, H. H. (2003). Indonesian Rainfall Variability: Impacts of ENSO and Local Air–Sea Interaction. *Journal of Climate*, *16*(11), 1775–1790. https://doi.org/10.1175/1520-0442(2003)016<1775:IRVIOE>2.0.CO;2

Hendon, H. H., Lim, E.-P., & Nguyen, H. (2014). Seasonal Variations of Subtropical Precipitation Associated with the Southern Annular Mode. *Journal of Climate*. https://doi.org/10.1175/JCLI-D-13-00550.1

Hersbach, H., Bell, B., Berrisford, P., Biavati, G., Horányi, A., Muñoz Sabater, J., Nicolas, J., Peubey, C., Radu, R., Schepers, D., Simmons, A., Soci, C., Dee, D., & Thépaut, J.-N. (2023). ERA5 monthly averaged data on single levels from 1940 to present. Copernicus Climate Change Service (C3S) Climate Data Store (CDS). https://doi.org/10.24381/CDS.F17050D7

Holgate, C. M., Evans, J. P., Dijk, A. I. J. M. v., Pitman, A. J., & Virgilio, G. D. (2020). Australian Precipitation Recycling and Evaporative Source Regions. *Journal of Climate*, *33*(20), 8721–8735. https://doi.org/10.1175/JCLI-D-19-0926.1

Hope, P. K., & Watterson, I. G. (2018). Persistence of cool conditions after heavy rain in australia. *Journal of Southern Hemisphere Earth Systems Science*, *68*(1), 41–64.

Hou, M., & Tang, Y. (2022). Recent progress in simulating two types of ENSO – from CMIP5 to CMIP6. *Frontiers in Marine Science*, *9*. Retrieved February 7, 2024, from https://www.frontiersin.org/articles/10.3389/fmars.2022.986780

Huang, A. T., Gillett, Z. E., & Taschetto, A. S. (2024). Australian Rainfall Increases During Multi-Year La Niña. *Geophysical Research Letters*, *51*(9), e2023GL106939. https://doi.org/10.1029/2023GL106939

Huang, B., Thorne, P. W., Banzon, V. F., Boyer, T., Chepurin, G., Lawrimore, J. H., Menne, M. J., Smith, T. M., Vose, R. S., & Zhang, H.-M. (2017). NOAA Extended Reconstructed Sea Surface Temperature (ERSST), Version 5 [Last Modified: 2023-06-23]. https://doi.org/10.7289/V5T72FNM

Huang, B., Angel, W., Boyer, T., Cheng, L., Chepurin, G., Freeman, E., Liu, C., & Zhang, H.-M. (2018). Evaluating sst analyses with independent ocean profile observations. *Journal of Climate*, *31*(13), 5015–5030. https://doi.org/10.1175/JCLI-D-17-0824.1

Hung, C.-W., & Yanai, M. (2004). Factors contributing to the onset of the Australian summer monsoon. *Quarterly Journal of the Royal Meteorological Society*, *130*(597), 739–758. https://doi.org/10.1256/qj.02.191

Hunt, K. M. R., & Turner, A. G. (2017). The Effect of Soil Moisture Perturbations on Indian Monsoon Depressions in a Numerical Weather Prediction Model. *Journal of Climate*, *30*(21), 8811–8823. https://doi.org/10.1175/JCLI-D-16-0733.1

Ida, I. P., Hartono, H., Sunarto, S., & Sopaheluwakan, A. (2020). The interaction between local factors and the convectively coupled equatorial waves over indonesia during the western north pacific and australian monsoon phase. *Meteorology Hydrology and Water Management*, *8*(1), 84–89. https://doi.org/10.26491/mhwm/117576

Jiang, W., Huang, P., Huang, G., & Ying, J. (2021). Origins of the Excessive Westward Extension of ENSO SST Simulated in CMIP5 and CMIP6 Models. *Journal of Climate*, *34*(8), 2839–2851. https://doi.org/10.1175/JCLI-D-20-0551.1

Kousky, V., & Higgins, R. (2007). An alert classification system for monitoring and assessing the enso cycle. *Weather and Forecasting*, *22*(2), 353–371.

Krishnamurti, T., Gentilli, J., & Smith, P. (2023, December). Monsoon | Meteorology, Climate & Effects. Retrieved December 14, 2023, from https://www.britannica.com/science/monsoon

Lawrence, D. M., Fisher, R. A., Koven, C. D., Oleson, K. W., Swenson, S. C., Bonan, G., Collier, N., Ghimire, B., van Kampenhout, L., Kennedy, D., et al. (2019). The community land model version 5: Description of new features, benchmarking, and impact of forcing uncertainty. *Journal of Advances in Modeling Earth Systems*, *11*(12), 4245–4287.

Lee, J.-Y., Marotzke, J., Bala, G., Cao, L., Corti, S., Dunne, J. P., Engelbrecht, F., Fischer, E., Fyfe, J. C., Jones, C., et al. (2021). Future global climate: Scenario-based projections and near-term information. In *Climate change 2021: The physical science basis. contribution of working group i to the sixth assessment report of the intergovernmental panel on climate change* (pp. 553–672). Cambridge University Press.

Lin, Z., & Li, Y. (2012). Remote influence of the tropical atlantic on the variability and trend in north west australia summer rainfall. *Journal of Climate*, *25*(7), 2408–2420. https://doi.org/https://doi.org/10.1175/JCLI-D-11-00020.1

Lopes, A. B., Andreoli, R. V., Souza, R. A. F., Cerón, W. L., Kayano, M. T., Canchala, T., & de Moraes, D. S. (2022). Multiyear La Niña effects on the precipitation in

South America. *International Journal of Climatology*, *42*(16), 9567–9582. https://doi.org/10.1002/joc.7847

Madden, R. A., & Julian, P. R. (1972). Description of Global-Scale Circulation Cells in the Tropics with a 40–50 Day Period. *Journal of the Atmospheric Sciences*, *29*(6), 1109–1123. https://doi.org/10.1175/1520-0469(1972)029<1109:DOGSCC>2.0.CO;2

Martius, O., Wehrli, K., & Rohrer, M. (2021). Local and remote atmospheric responses to soil moisture anomalies in australia. *Journal of Climate*, *34*(22), 9115–9131.

McBride, J. L., & Nicholls, N. (1983). Seasonal Relationships between Australian Rainfall and the Southern Oscillation. *Monthly Weather Review*, *111*(10), 1998–2004. https://doi.org/10.1175/1520-0493(1983)111<1998:SRBARA>2.0.CO;2

McGregor, S., Gallant, A., & van Rensch, P. (2024). Quantifying ensos impact on australia's regional monthly rainfall risk. *Geophysical Research Letters*, *51*(6), e2023GL106298.

Mollah, W. S., & Cook, I. M. (1996). Rainfall variability and agriculture in the semi-arid tropics—the Northern Territory, Australia. *Agricultural and Forest Meteorology*, *79*(1), 39–60. https://doi.org/10.1016/0168-1923(95)02267-8

Narsey, S. Y., Brown, J. R., Colman, R. A., Delage, F., Power, S. B., Moise, A. F., & Zhang, H. (2020). Climate Change Projections for the Australian Monsoon From CMIP6 Models. *Geophysical Research Letters*, *47*(13). https://doi.org/10.1029/2019GL086816

Narsey, S., Reeder, M. J., Ackerley, D., & Jakob, C. (2017). A midlatitude influence on australian monsoon bursts. *Journal of Climate*, *30*, 5377–5393. https://api.semanticscholar.org/CorpusID:133341069

NOAA. (2023). Historical El Nino / La Nina episodes (1950-present). Retrieved February 2, 2024, from https://origin.cpc.ncep.noaa.gov/products/analysis_monitoring/ensostuff/ONI_v5.php

Okumura, Y. M., & Deser, C. (2010). Asymmetry in the duration of el niño and la niña. *Journal of Climate*, *23*(21), 5826–5843. https://doi.org/10.1175/2010JCLI3592.1

Okumura, Y. M., DiNezio, P., & Deser, C. (2017). Evolving Impacts of Multiyear La Niña Events on Atmospheric Circulation and U.S. Drought. *Geophysical Research Letters*, *44*(22), 11, 614–11, 623. https://doi.org/10.1002/2017GL075034

Planton, Y. Y., Guilyardi, E., Wittenberg, A. T., Lee, J., Gleckler, P. J., Bayr, T., McGregor, S., McPhaden, M. J., Power, S., Roehrig, R., et al. (2021). Evaluating climate models with the clivar 2020 enso metrics package. *Bulletin of the American Meteorological Society*, *102*(2), E193–E217.

Power, S., Casey, T., Folland, C., Colman, A., & Mehta, V. (1999). Inter-decadal modulation of the impact of ENSO on Australia. *Climate Dynamics*, *15*(5), 319–324. https://doi.org/10.1007/s003820050284

Power, S., Haylock, M., Colman, R., & Wang, X. (2006). The predictability of interdecadal changes in enso activity and enso teleconnections. *Journal of Climate*, *19*(19), 4755–4771.

Rahmati, M., Amelung, W., Brogi, C., Dari, J., Flammini, A., Bogena, H., Brocca, L., Chen, H., Groh, J., Koster, R. D., et al. (2024). Soil moisture memory: State-of-the-art and the way forward. *Reviews of Geophysics*, *62*(2), e2023RG000828.

Rashid, H. A., Sullivan, A., Dix, M., Bi, D., Mackallah, C., Ziehn, T., Dobrohotoff, P., O'Farrell, S., Harman, I. N., Bodman, R., et al. (2022). Evaluation of climate variability and change in ACCESS historical simulations for CMIP6. *Journal of Southern Hemisphere Earth Systems Science*, *72*(2), 73–92.

Roxy, M., Dasgupta, P., McPhaden, M. J., Suematsu, T., Zhang, C., & Kim, D. (2019). Twofold expansion of the Indo-Pacific warm pool warps the MJO life cycle. *Nature*, *575*(7784), 647–651.

Sekizawa, S., Nakamura, H., & Kosaka, Y. (2018). Interannual Variability of the Australian Summer Monsoon System Internally Sustained Through Wind - Evaporation Feedback. *Geophysical Research Letters*, *45*(15), 7748–7755. https://doi.org/10.1029/2018GL078536

Sekizawa, S., Nakamura, H., & Kosaka, Y. (2021). Remote Influence of the Interannual Variability of the Australian Summer Monsoon on Wintertime Climate in East Asia and the Western North Pacific [Publisher: American Meteorological Society Section: Journal of Climate]. *Journal of Climate*, *34*(23), 9551–9570. https://doi.org/10.1175/JCLI-D-21-0202.1

Sekizawa, S., Nakamura, H., & Kosaka, Y. (2023). Interannual Variability of the Australian Summer Monsoon Sustained through Internal Processes: Wind - Evaporation Feedback, Dynamical Air–Sea Interaction, and Soil Moisture Memory. *Journal of Climate*, *36*(3), 983–1000. https://doi.org/10.1175/JCLI-D-22-0116.1

Sharmila, S., & Hendon, H. H. (2020). Mechanisms of multiyear variations of Northern Australia wet-season rainfall. *Scientific Reports*, *10*(1), 5086. https://doi.org/10.1038/s41598-020-61482-5

Taschetto, A. S., Ummenhofer, C. C., Sen Gupta, A., & England, M. H. (2009). Effect of anomalous warming in the central Pacific on the Australian monsoon. *Geophysical Research Letters*, *36*(12). https://doi.org/10.1029/2009GL038416

Taschetto, A. S., & England, M. H. (2009). El Niño Modoki Impacts on Australian Rainfall. *Journal of Climate*, *22*(11), 3167–3174. https://doi.org/10.1175/2008JCLI2589.1

Taschetto, A. S., Gupta, A. S., Hendon, H. H., Ummenhofer, C. C., & England, M. H. (2011). The Contribution of Indian Ocean Sea Surface Temperature Anomalies on Australian Summer Rainfall during El Niño Events. *Journal of Climate*, *24*(14), 3734–3747. https://doi.org/10.1175/2011JCLI3885.1

Taschetto, A. S., Haarsma, R. J., Gupta, A. S., Ummenhofer, C. C., Hill, K. J., & England, M. H. (2010). Australian Monsoon Variability Driven by a Gill–Matsuno-Type Response to Central West Pacific Warming [Publisher: American Meteorological Society Section: Journal of Climate]. *Journal of Climate*, *23*(18), 4717–4736. https://doi.org/10.1175/2010JCLI3474.1

Tatebe, H., & Watanabe, M. (2018). MIROC MIROC6 model output prepared for CMIP6 CMIP piControl. https://doi.org/10.22033/ESGF/CMIP6.5711

Timbal, B., Power, S., Colman, R., Viviand, J., & Lirola, S. (2002). Does soil moisture influence climate variability and predictability over australia? *Journal of Climate*, *15*(10), 1230–1238.

Titchner, H. A., & Rayner, N. A. (2014). The Met Office Hadley Centre sea ice and sea surface temperature data set, version 2: 1. Sea ice concentrations [_eprint: https://onlinelibrary.wiley.com/doi/pdf/10.1002/2013JD020316]. *Journal of Geophysical Research: Atmospheres*, *119*(6), 2864–2889. https://doi.org/10.1002/2013JD020316

Tozer, C. R., Risbey, J. S., Monselesan, D. P., Pook, M. J., Irving, D., Ramesh, N., Reddy, J., & Squire, D. T. (2023). Impacts of enso on australian rainfall: What not to expect. *Journal of Southern Hemisphere Earth Systems Science*, *73*(1), 77–81.

Uehling, J., & Misra, V. (2020). Characterizing the Seasonal Cycle of the Northern Australian Rainy Season. *Journal of Climate*, *33*(20), 8957–8973. https://doi.org/10.1175/JCLI-D-19-0592.1

Wu, X., Okumura, Y. M., & DiNezio, P. N. (2019). What Controls the Duration of El Niño and La Niña Events? *Journal of Climate*, *32*(18), 5941–5965. https://doi.org/10.1175/JCLI-D-18-0681.1

Yu, Y., & Notaro, M. (2020). Observed land surface feedbacks on the Australian monsoon system. *Climate Dynamics*, *54*(5), 3021–3040. https://doi.org/10.1007/s00382-020-05154-0

Zhao, Y., & Sun, D.-Z. (2022). ENSO Asymmetry in CMIP6 Models [Publisher: American Meteorological Society Section: Journal of Climate]. *Journal of Climate*, *35*(17), 5555–5572. https://doi.org/10.1175/JCLI-D-21-0835.1

Zheng, T., Feng, T., Xu, K., & Cheng, X. (2020). Precipitation and the associated moist static energy budget off western australia in conjunction with ningaloo niño. *Frontiers in Earth Science*, *8*, 597915.

Declaration of consent

on the basis of Article 30 of the RSL Phil.-nat. 18

Name/First Name: Rossier Quentin

Registration Number: 19-400-522

Study program: Climate Sciences

Bachelor ☐ Master ☑ Dissertation ☐

Title of the thesis: Influence of multi-year La Niña and soil moisture feedback on the Australian Monsoon

Supervisor: Prof. Dr.Stefan Brönnimann

I declare herewith that this thesis is my own work and that I have not used any sources other than those stated. I have indicated the adoption of quotations as well as thoughts taken from other authors as such in the thesis. I am aware that the Senate pursuant to Article 36 paragraph 1 litera r of the University Act of 5 September, 1996 is authorized to revoke the title awarded on the basis of this thesis.

For the purposes of evaluation and verification of compliance with the declaration of originality and the regulations governing plagiarism, I hereby grant the University of Bern the right to process my personal data and to perform the acts of use this requires, in particular, to reproduce the written thesis and to store it permanently in a database, and to use said database, or to make said database available, to enable comparison with future theses submitted by others.

Sydney, 20.08.2024

Place/Date

Signature